AD-A109 486 NAVAL OCEAN SYSTEMS CENTER SAN DIEGO CA F/G 22/2
SATELLITE-BORNE 'NON-DOD SENSORS' FOR TERRESTRIAL OBSERVATIONS.(U)
AUG 81 H M WIGHT
UNCLASSIFIED NOSC/TD-458 NL

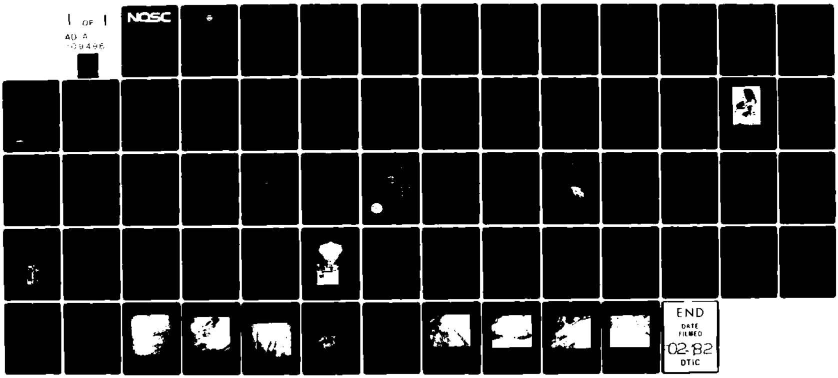

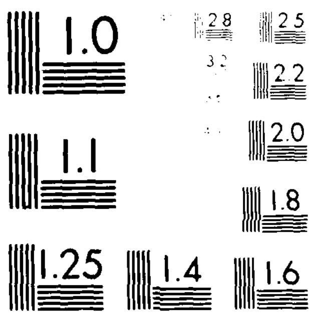

MICROCOPY RESOLUTION TEST CHART

(12) LEVEL

NOSC

AD A109486

NOSC TD 458

Technical Document 458

SATELLITE-BORNE "NON-DoD SENSORS" FOR TERRESTRIAL OBSERVATIONS

H.M. Wight

August 1981

NAVAL OCEAN SYSTEMS CENTER
SAN DIEGO, CALIFORNIA 92152

NAVAL OCEAN SYSTEMS CENTER, SAN DIEGO, CA 92152

AN ACTIVITY OF THE NAVAL MATERIAL COMMAND

SL GUILLE, CAPT, USN
Commander

HL BLOOD
Technical Director

ADMINISTRATIVE INFORMATION

The work covered by this report was sponsored by Naval Operations, under the direction of CAPT D. W. Holsten, NOP 940D, and accomplished during fiscal year 1981.

Released by
M. R. Akers, Head
Systems Concepts and
Analysis Division

Under authority of
E. B. Tunstall, Head
Surveillance Systems
Department

UNCLASSIFIED

SECURITY CLASSIFICATION OF THIS PAGE (When Data Entered)

REPORT DOCUMENTATION PAGE		READ INSTRUCTIONS BEFORE COMPLETING FORM
1. REPORT NUMBER NOSC Technical Document 458 (TD 458)	2. GOVT ACCESSION NO. AD-A109486	3. RECIPIENT'S CATALOG NUMBER
4. TITLE (and Subtitle) SATELLITE-BORNE "NON-DoD SENSORS" FOR TERRESTRIAL OBSERVATIONS		5. TYPE OF REPORT & PERIOD COVERED Fiscal Year 1981
		6. PERFORMING ORG. REPORT NUMBER
7. AUTHOR(s) H. M. Wight		8. CONTRACT OR GRANT NUMBER(s)
9. PERFORMING ORGANIZATION NAME AND ADDRESS Naval Ocean Systems Center San Diego, CA 92152		10. PROGRAM ELEMENT, PROJECT, TASK AREA & WORK UNIT NUMBERS
11. CONTROLLING OFFICE NAME AND ADDRESS		12. REPORT DATE August 1981
		13. NUMBER OF PAGES 60
14. MONITORING AGENCY NAME & ADDRESS(if different from Controlling Office)		15. SECURITY CLASS. (of this report) Unclassified
		15a. DECLASSIFICATION/DOWNGRADING SCHEDULE

16. DISTRIBUTION STATEMENT (of this Report)

Approved for public release; distribution unlimited

17. DISTRIBUTION STATEMENT (of the abstract entered in Block 20, if different from Report)

18. SUPPLEMENTARY NOTES

19. KEY WORDS (Continue on reverse side if necessary and identify by block number)

Non DoD Sensors
Satellite Sensors
Remote Terrestrial Sensing
NASA Terrestrial Sensors

20. ABSTRACT (Continue on reverse side if necessary and identify by block number)

This is a summary review that was made of satellite-borne "non-DoD sensors" used for terrestrial observations. The term non-DoD sensors refers to "civil" (as contrasted with "military") remote sensing systems. The civil satellite-borne sensing systems were developed for the most part by NASA and are employed operationally by NOAA/NESS.

DD FORM 1 JAN 73 1473 EDITION OF 1 NOV 65 IS OBSOLETE
S/N 0102-LF-014-6601

UNCLASSIFIED

SECURITY CLASSIFICATION OF THIS PAGE (When Data Entered)

UNCLASSIFIED
SECURITY CLASSIFICATION OF THIS PAGE (When Data Entered)

UNCLASSIFIED
SECURITY CLASSIFICATION OF THIS PAGE(When Data Entered)

EXECUTIVE SUMMARY

This is a summary review that was made of satellite-borne "non-DoD sensors" used for terrestrial observations. The term "non-DoD sensors" refers to "civil" (as contrasted with "military") remote sensing systems. The civil satellite-borne sensing systems were developed for the most part by NASA and are employed "operationally" by NOAA/NESS.

An ultimate goal (of the preliminary, initial effort) will be the identification of promising civil sensors, experience and associated technology which could be utilized profitably by the U.S. Navy in the area of ocean surveillance. Summary information is presented concerning the NIMBUS, LANDSAT, TIROS and GOES programs. Satellite-borne sensors for earth viewing – image forming, operating in the visible/IR and microwave portions of the EM spectrum, are also summarized.

PREFACE

The author makes no claim for originality in this document. Most of the material contained herein was adapted from the many sources listed in the bibliography.

GLOSSARY OF ACRONYMS AND ABBREVIATIONS

A/D	Analog-to-Digital
AF	Audio Frequency, Air Force
AFB	Air Force Base
AM	Amplitude Modulation, Ante Meridian
APL	Applied Physics Laboratory
APT	Automatic Picture Transmission
AVCS	Advanced Vidicon Camera System
AVHRR	Advanced Very High Resolution Radiometer
BCD	Binary Coded Decimal
bps	Bits per second
°C	Degrees Centigrade
CCD	Charged Coupled Device
CDHS	Communications and Data Handling Subsystem
CDIU	Command and Data Interface Unit
CID	Charge Injection Device
cm	Centimeter
CO_2	Carbon Dioxide
CRT	Cathode Ray Tube
CZCS	Coastal Zone Color Scanner
D/A	Digital-to-Analog
dB	Decibel
DCS	Data Collection System
DEMUX	Demultiplex
DIP	Digital Information Processor
DMSP	Defense Meteorological Satellite Program
DoD	Department of Defense
DPS	Data Processing System
EM	Electromagnetic
ERBE	Earth Radiation Budget Experiment
EROS	Earth Resources Observation System
ERTS	Earth Resources Technology Satellite
ESA	European Space Agency
ESS	Environmental Satellite Survey
ESSA	Environmental Sciences Services Administration
ETR	Eastern Test Range (Cape Canaveral, Florida)

FDM	Frequency Division Multiplex
FIR	Far IR
FM	Frequency Modulation
FNOC	Fleet Numerical Oceanographic Center
FNWC	Fleet Numerical Weather Central (Currently, FNOC)
FOV	Field of View
FSK	Frequency Shift Keying
GARP	Global Atmospheric Research Program
GE	General Electric Company
GHz	Gigahertz (10^9 cycles/second)
GOES	Geostationary Operational Environmental Satellite
GSFC	Goddard Space Flight Center (Greenbelt, Maryland)
HAC	Hughes Aircraft Company
HF	High Frequency
(Hg Cd) Te	Mercury Cadmium Telluride
HIRS	High Resolution Infrared Radiation Sounder
HRPT	High Resolution Picture Transmission
Hz	Hertz (cycles per second)
IEEE	Institute of Electrical and Electronic Engineers
I/F	Interface
IFOV	Instantaneous Field of View
InSb	Indium Antimonide
I/O	Input/Output
ips	Inches per second
IR	Infrared
ITOS	Improved TIROS Operational System
JPL	Jet Propulsion Laboratory
°K	Degrees Kelvin
kbps	Kilobits per second
kHz	Kilohertz (10^3 cycles/second)
kms	Kilometers
LANDSAT	Land Satellite
LaRC	Langley Research Center (Hampton, Virginia)

LIDAR	Light Detection and Ranging
LIMS	LIMB IR Monitoring of the Stratosphere
LOS	Line-of-Sight
L/V	*Launch Vehicle*
MLA	Multispectral Linear Array
mm	Millimeter
MOS	Metal Oxide Silicon
mrad	Milliradian
MS	Microwave Scatterometer
ms	Millisecond
MSS	Multispectral Scanner
MUX	Multiplexer
NASA	National Aeronautics and Space Administration
NESS	National Environmental Satellite Service
NETD or	
NEΔT	Noise-Equivalent Temperature Difference
NIMBUS	Program Named for Rain Cloud (from the Latin)
NIR	Near IR
nm	*Nautical Mile or Nanometer* (10^{-9} *cm*)
NOAA	National Oceanic and Atmospheric Administration
NOSS	National Oceanic Satellite Service
PAM	Phase Amplitude Modulation
PCM	Pulse Code Modulation
PFM	Pulse Frequency Modulation
Pixel	Picture Element
PM	Phase Modulation, Post Meridian
PMEL	Pacific Marine Environmental Laboratory (Seattle, Washington)
PPS	Pulses Per Second
PSK	Phase Shift Keying
Rad	Radian
Radar	Radio Detection and Ranging
RBV	Return Beam Vidicon
RCA	Radio Corporation of America
RF	Radio Frequency

SAMS	Stratospheric and Mesospheric Sounder (Experiment) (Currently USAF Space Div.)
SAMSO	Space and Missile System Organization
SBUV/TON	Solar Backscatter Ultraviolet/Total Ozone Mapping Spectrometer (Experiment)
SAR	Synthetic Aperture Radar
SBRC	Santa Barbara Research Center (Part of HAC)
SEM	Space Environment Monitor
SEMS	Space Environmental Monitor System
SIO	Scripps Institution of Oceanography
SIRS	Satellite IR Spectrometer
SMIRR	Shuttle Multispectral IR Reflectance Radiometer
SMMR	Scanning Multichannel Microwave Radiometer
SNR	Signal-to-Noise Ratio
SOSS	Satellite Ocean Surveillance System
SSU	Stratospheric Sounder Unit
SWIR	Short Wavelength IR
THIR	Temperature and Humidity IR Radiometer
TIP	TIROS Information Processor
TIROS	Television IR Observatory Satellite
TM	Thematic Mapper
TOVS	Tiros Operational Vertical Sounder
TV	Television
TWERLE	Tropical Wind, Energy Conversion and Reference Level Experiment
UCSD	University of California at San Diego
UHF	Ultra-High Frequency
UV	Ultraviolet
VAS	Visible and IR Spin Scan Radiometer and Atmospheric Sounder
VHF	Very High Frequency
VIP	Versatile Information Processor
W	Watts
Wcm^{-2}	Watts per square centimeter
Wm^{-2}	Watts per square meter
WTR	Western Test Range, Vandenberg AFB, California
WWW	World Weather Watch
μ	Micron (10^{-6} meters)
μm	Micrometer (10^{-6} meters)
λ	Wavelength

CONTENTS

ILLUSTRATIONS

TABLES

1.0 INTRODUCTORY COMMENTS

This document presents an initial survey and review of civil, i.e., *non-DoD sensor systems*, aboard satellites for remote sensing of the earth's surface. The sensors involved (multi-spectral visible/IR radiometric scanners, multichannel microwave radiometric scanners and synthetic aperture radar) were developed initially by NASA (or under its direct sponsorship) and utilized operationally by NOAA/NESS.

The ultimate goal of the present effort is to assess and identify the possible benefits for the U.S. Navy in the area of technology transfer based on civil remote sensing system experience. Specifically such technology transfer would be directed toward aiding in the accomplishment of the U.S. Navy's satellite ocean surveillance missions.

Non-DoD satellite-borne earth sensing systems primarily have emphasized image mapping of the earth's surface and the generation of large scale synoptic meteorological data (e.g., cloud cover associated with storm fronts). LANDSAT and SEASAT-A sensors are of particular interest in the context of the present review.

The basic difference between DoD and non-DoD remote sensing missions has influenced the somewhat divergent development trends for sensor systems in the two domains (military vs civil). DoD remote sensing systems usually have required rapid detection, localization, classification and identification of potentially hostile threat targets (missiles, aircraft, surface naval ships, etc.), often under poor weather conditions on a 24-hour per day basis. Civil applications usually do not require such a rapid "real-time" response for the processing and imaging of phenomena on the earth's surface. Many of the civil data acquired are processed on a relatively leisurely basis and then archived for future use. The daily acquisition data rate generated by the LANDSAT MSS (multispectral scanner) is very large, of the order of 10^{10} bits. The resolution size for MSS images is roughly 80m. Many satellite generated meteorological pictures have a resolution size of several km (such a large resolution gain size would very likely preclude classification of a military platform of interest).

For the readers' benefit, the ultimate goal of this report and potential follow-on work is illustrated in Figure 1. Civil applications involving remote sensing of the earth from satellites include oceanography, meteorology, agriculture and forestry, geology, geodesy, hydrology, large scale polution monitoring, ecology and land use, etc.

Remote sensing from satellites has reached such a state of maturity that it is currently treated in university courses (e.g., UCSD Extension Course No. 823.4 winter quarter, titled "Land and Sea Applications of Remote Sensing from Satellites").

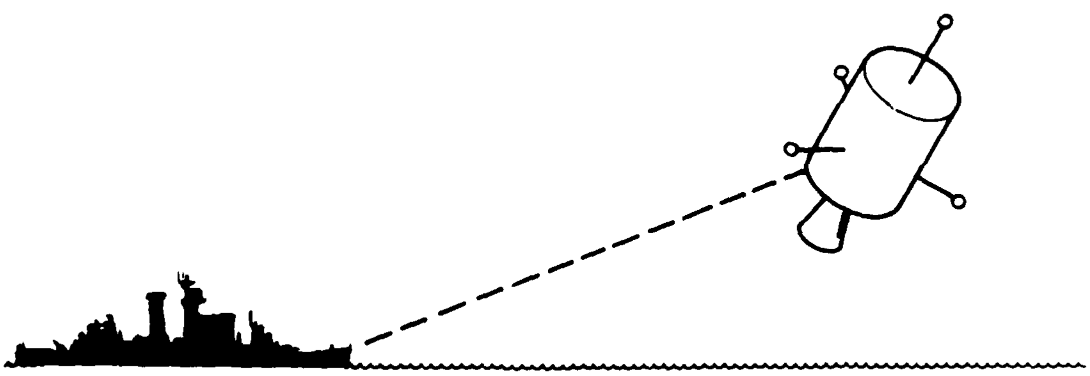

Figure 1. Ocean surveillance by remote sensing.

2.0 BACKGROUND INFORMATION

The remote sensors of interest in the present survey have been carried aboard spacecraft satellites launched for the NIMBUS, LANDSAT, TIROS and GOES projects. The National Aeronautics and Space Administration (NASA) R&D projects are managed by NASA's Office of Space and Terrestrial Applications. Project management is centered in NASA GSFC (Goddard Space Flight Center) in Greenbelt, Maryland. Certain follow-on operational satellite systems, evolving from the original NASA R&D efforts (such as TIROS and GOES), are managed by NOAA/NESS (National Oceanic and Atmospheric Agency/ National Environmental Satellite System) which is headquartered in Suitland, Maryland. NASA and NOAA/NESS have had a close working relationship over the past 20 years. The operational responsibility for certain systems, such as LANDSAT, has remained with NASA.

2.1 NIMBUS

The NIMBUS (Latin for "rain cloud") program originated at NASA in the early 1960s as a series of R&D earth-sensing spacecraft and associated sensor systems. NIMBUS has served in the role of a test bed for many of the sensors later flown on TIROS, GOES, DMSP and SEASAT satellites. The space division of the General Electric Company (Valley Forge, Pennsylvania) has been the prime contractor for the NIMBUS program.

The general objectives of the NIMBUS program were to:

1. Develop advanced passive radiometric and spectrometric sensors for daily global surveillance of the earth's atmosphere to provide a data base for long-range weather forecasting
2. Develop and evaluate new active and passive sensors for sounding the earth's atmosphere and mapping both land and water surface characteristics
3. Develop advanced space technology and ground techniques for meteorological and earth-observational spacecraft
4. Develop new techniques and knowledge useful for the exploration of other planetary atmospheres
5. Participate in global observation programs (World Weather Watch) by expanding daily global weather observation capability
6. Provide a supplemental source of operational meteorological data

Seven NIMBUS spacecraft were launched during the course of the program. They were:

- NIMBUS-1 August 1964
- NIMBUS-2 May 1966
- NIMBUS-3 April 1969
- NIMBUS-4 April 1970
- NIMBUS-5 December 1972
- NIMBUS-6 June 1975
- NIMBUS-7 September 1978

All of the above launches were in polar orbit from NASA's Western Test Range (Vandenberg AFB, California).

During the evolution of the program the sensor/data telemetering system payload gradually increased from 100 pounds (NIMBUS-1) to roughly 600 pounds (NIMBUS-7). Table 1 summarizes the various experiments and associated sensors flown during the NIMBUS program.

Abbreviation	Experiment Name	Experimenter	Equipment Contractor	Type of Sensor	Scientific Objective	Special Instrument Technique	Number of Data Channels (Sensor Only)	Spectral Interval	Pointing Direction	Angular Resolution (Degrees)	Scanning	Nimbus Spacecraft
APT	Automatic Picture Taking	GSFC	RCA	Slow Readout Vidicon Camera	Local Cloud Cover Images (pictures)	Stored Image Vidicon (slow scan)	1	0.5 to 0.75 µm	Nadir	2.5 nm**	77°	1, 2
AVCS	Advanced Vidicon Camera	GSFC	RCA	Wide Angle Multi-vidicon Camera	High Resolution Cloud ver Images	Vidicon Camera	3	0.5 to 0.75 µm	Nadir	1.0 nm**	107°	1, 2
BUV	Backscatter Ultraviolet Spectrometer	NCAR/GSFC	Beckman	Radiometer/ Spectrometer	Spatial Distribution of Atmospheric Ozone	Grating Spectrometer	12	2500 to 3888 Å	Nadir	12.0	None	4
CZCS	Coastal Zone Color Scanner	GSFC	Ball Bros	Multispectral Imaging Radiometer	Ocean and Coastal Area Measurement of Chlorophyll, Vegetation, Temp. and Gelbstoff	Mechanically Scanned Radiometer	6	433 to 800 µm 10.5 to 12.5 µm	Nadir	0.05	Across Track ±40° Along Track ±20	7
ESMR	Electrically Scanning Microwave Radiometer	GSFC	Aerojet	Scanning (imaging) Microwave Radiometer	Thermal Image of the Earth and Ocean Unobscured by Clouds	Electronically Scanned Phased Array Antenna Dicke Switch	1	19.35 GHz	Nadir	1.4	74°	5
ESMR-F	Electrically Scanning Microwave Radiometer	GSFC	Aerojet	Two Polarization, Scanning Microwave Radiometer	Map Liquid Water Content of Clouds Sea-Ice Cover, Gross Characteristics of Land	Electronic Conical Scanned Phased Array Antenna Measure both Horizontal and Vertical Simultaneously Dicke	2	37 GHz	Nadir	1.1	74°	6
ERB	Earth Radiation Budget	NOAA	Gulton	Fixed and Scanning Radiometer	Measure Planetary Heat Budget total Solar Radiation and Angular Distribution of Earth Flux	Two Axis Gimbal Mounted Scanning Radiometer	22	2000 Å – 50 µm	Nadir and Towards the Sun	5.14 x +0.25 Scan Channels 1.5 Fixed Channels	Horizon to Horizon, Along Track and Across Track	6, 7
FWS	Filter Wedge Spectrometer	GSFC	ITT	Radiometer/ Spectrometer	Vertical Distribution and Temperature Profile of Water Vapor and Carbon Dioxide	Continuously Variable Interference Filter Disk	1	1.2 – 2.4 µm 3.2 – 6.4 µm	Nadir	2.6	None	4
HIRS	High Resolution Temperature Sounder	GSFC/NOAA	ITT	Scanning Spectral Radiometer	Vertical Temperature Profile and H_2O Distribution	Mechanically Scanned Radiometer with Spectral Selection by Interference Filters – Radiation Cooler	17	0.7 – 15 µm	Nadir	1.5	72°	6
HRIR	High Resolution Infrared Radiometer	GSFC	ITT	IR Imaging Radiometer	Night Cloud Cover	Mechanically Scanned Imaging Radiometer	1	3.4 to 4.2 µm	Nadir	0.5	Horizon to Horizon	1, 2
				Dual Channel Imaging Radiometer	Day/Night Cloud Cover	Spectral Dispersion by Interference Filters	2	3.4 to 4.2 µm 0.7 to 1.3 µm	Nadir	0.4		3
IDCS	Image Dissector Camera	GSFC	ITT	Imaging Radiometer	Day Cloud Cover	Electrically Scanned Imaging Radiometer	1	0.5 to 0.75 µm	Nadir	1.2 nm**	98.2°	3, 4
IRIS	Infrared Interferometer Spectrometer	GSFC	TI	Radiometer/ Spectrometer	Vertical Temperature & Moisture Profile and Distribution of Other Atmospheric Gases	Michelson Interferometer with Self Calibration	1	5 to 25 µm	Nadir	8.0	None	3
										5.0		4
IRLS	Interrogation, Recording, and Location System	GSFC	Radiation Inc		Locate, Interrogate and Record Data from Remote Stations (balloons and buoys)				Nadir	120.0 (beamwidth)	None	3, 4
ITPR	Infrared Temperature Profile Radiometer	ESSA	Gulton	Radiometer/ Spectrometer	Vertical Temperature Profile (CO_2)	Fixed Spectral Filters Mech. Step Scan	7	[illegible] to 15 µm	Nadir	1.5	76°	5
LIMS	Limb Infrared Monitoring of the Stratosphere	LRC	Honeywell	Multispectral Scanning Radiometer	Stratospheric Measurement of Temp., Ozone, Water Vapor, Nitric Acid, Nitrogen Dioxide	Mechanical Scanning Radiometer	6	6.1 to 15.8 µm	Earth Limb	0.03°	Horizon to Space 12°	7
LRIR	Limb Radiance Inversion Radiometer	NCAR/U. of Florida	Honeywell	Scanning Spectral Radiometer	Stratospheric Measurements of Temperatures, Water Vapor and Ozone Profiles	Mechanically Scanned Radiometer Interference Filters CH_3/NH_3 Cryo Cooler	4	8.? – 25 µm	Towards the Horizon	0.3 x 0.03	10° Acquisition 2° Track Vertically	6
MRIR	Medium Resolution Infrared Radiometer	GSFC	SBRC	Imaging Radiometer/ Spectrometer	Vertical Temperature Profile, Heat Balance, and Distribution of Atmospheric Gases	Mechanically Scanned Radiometer with Fixed Interference Filters	5	0.5 to 29 µm	Nadir	2.7	Horizon to Horizon	2, 3
MUSE	Monitor Ultraviolet Solar Energy	GSFC	Adcole	Radiometer/ Spectrometer	Measurement of Solar Ultraviolet Energy	Fixed Spectral Filter	5	1120 to 3100 Å	Towards Sun	90	None	3, 4
NEMS	Microwave Spectrometer	JPL/MIT	JPL	Radiometer/ Spectrometer	Vertical Temperature Profile Using O_2 Line, Water and Water Vapor Distribution	Microwave Radiometer (Dicke Superheterodyne)	5	20 to 60 GHz	Nadir	10.0	None	5
PMR	Pressure Modulated Radiometer	Oxford	Marconi	Scanning Spectral Radiometer	Vertical Temperature Profiles to 85 KM	Pressure Broadening Spectral Filter	2	15 µm	Nadir	4.0 x 20.0	15°	6
RMP	Rate Monitoring Package	GSFC	Sperry		Measurement of Angular Rate by Gas Bearing Gyro	Hydrodynamic Gas Bearing Gyroscope					None	3
RTG	Radioisotope Thermoelectric Generator	AEC	Martin		Assess the Usefulness of Radioactive Power Supplies						None	3
SAM II	Stratospheric Aerosol Measurement II	LRC	University of Wyoming	Spectral Radiometer	Measure and Map Global Aerosol Concentration and Optical Properties in Stratosphere and Troposphere	Mechanically Scanned Radiometer	1	1 µm	Spacecraft Sunrise/Sunset	0.01°	10° Vertical Scan	7
SAMS	Stratospheric and Mesospheric Sounder	Oxford	Hawker Siddley	Pressure Broadening Spectral Radiometer	Global Measurement of Temperature and Select Gaseous Distribution	Mechanically Scanned Radiometer	9	2.7 to 15 µm 25 to 100 µm	Towards Horizon	1.6° x 16°	Horizon +5° to 9, ±15° About	7
SBUV/TOMS	Solar Backscatter UV Energy and Total Ozone Mapping Spectrometer	GSFC	Beckman	Monochro Monitor Photometer	Map Total and Vertical Distribution of Ozone, Measure Solar Irradiance	Fixed and Spectral Scanning Radiometers (TOMS SBUV)	20	16 µm to 80 µm	Nadir	SBUV 11° TOMS 3°	Vertical and Cross Track	7
SCAMS	Scanning Microwave Spectrometer	JPL/MIT	JPL	Scanning Spectral Radiometer	Vertical Temperature Using O_2 line, Water Vapor Distribution	Mechanically Scanned Microwave Radiometer (Dicke Superheterodyne)	5	20 – 60 GHz	Nadir	7.5	86°	6
SCMR	Surface Composition Mapping Radiometer	GSFC	ITT	Imaging Radiometer, Spectrometer	Identification of Surface Minerals (ERS)	Spectral Filters and Cooled Detector	3	0.8 to 1.1 µm 8.3 to 9.2 µm 10.5 to 11.3 µm (Far IR & Visible)	Nadir	[illegible]	Horizon to Horizon	5
SCR	Selective Chopper Radiometer	Reading & Oxford University	Marconi	Radiometer Spectrometer	Vertical Temperature Profile and Distribution of Atmospheric Gases	Selective Absorption of Gas	6	2 to 200 µm (Near to Very Far IR)	Nadir	1.0 & 5.0	None	4
							16			1.5 & 2.2		5
SMMR	Scanning Multichannel Microwave Radiometer	GSFC	JPL	Scanning Microwave Radiometer	Sea Temp., Surface Winds, Ice Extent, Soil Moisture, Snow Cover, Continental Ice, Atmospheric Moisture, Water Vapor and Rainfall	Mechanically Scanned Radiometer	10	6.6, 10.69, 18.0, 21.00, 37.00 GHz	42° Conical Off Nadir	0.8° – 4.2°	Conical Forward of Nadir ±2°	7
SIRS	Satellite Infrared Spectrometer	ESSA	ESSA	Radiometer Spectrometer	Vertical Temperature Profile and Distribution of Atmospheric Gases	Grating Spectrometer	8	11 to 15 µm (Far IR)	Nadir	[illegible]	None	3
			Gulton/SBRC				14	[illegible] µm (Far IR)			35	4
TADRE	Tracking and Data Relay Experiment	GSFC	GSFC/GE, BBC	S Band Transponder	Range and Range Rate Measurements, Data Relay	Doppler Shift			Zenith			4
THIR	Temperature/Humidity Infrared Radiometer	GSFC	SBRC	Imaging Radiometer Spectrometer	Cloud Cover and Water Vapor Mapping	Mechanically Scanned Radiometer		6.5 to [illegible] µm (Far IR)	Nadir	[illegible]	Horizon to Horizon	4, 5, 6, 7
								10.5 to 12.5 µm (Far IR)		[illegible]		
TWERLE	Tropical Winds Energy Conversion Reference Level Experiment	GSFC Univ. of Wisconsin	TI	RF Receiver Balloon Transmitter	Measure Large Scale Atmospheric Motions, Conversion of Potential to Kinetic Energy, Provide [illegible]	Antenna Receiver and Random Access Computer	8	400 MHz				6

**In Nautical Miles for 600 NM Orbit Altitude

Table 1. NIMBUS experiment summary.

Details of the final NIMBUS spacecraft, NIMBUS-7, and its sensor package are summarized below. NIMBUS-7 data products and their users are summarized in Table 2; Figure 2 depicts the NIMBUS-7 spacecraft. NIMBUS-7 represented a $79M effort.

NIMBUS-7 mission objectives were to:

1. Provide additional and new meteorological data in support of the Global Atmospheric Research Program (GARP)
   a. Earth radiation budget; solar inputs and earth reflected
   b. Global monitor of gases and temperature in stratosphere, within troposphere and mesopheric regions
   c. Measurement of aerosol atmospheric contamination
2. Provide new and additional oceanographic data, relating to:
   a. Chlorophyll concentration
   b. Sediment distribution
   c. Salinity concentration via Gelbstoffe determination
   d. Coastal and open water temperature

Sensor	Film and Tape Output Products	Scientific Parameters	Applications	Users
ERB	Daily, monthly and seasonal world grids Monthly and seasonal contour maps Zonal statistics	Earth fluxes Solar fluxes Zonal insolation	Climatology Ocean/atmosphere dynamics Weather modeling Terrestrial reflectance studies	GSFC, NOAA, LaRC CSU Drexel U of C (Davis) Eppley Lab Cal Tech
SMMR	Orbital Observations Bi-daily and monthly color contour maps	SEA/ICE parameters Ocean surface conditions Atmospheric conditions Land parameters Glacial features	Ocean dynamics Ice dynamics Ocean/atmosphere interactions Cryospheric dynamics Climatology and weather modelling	GSFC, MIT, U of Wash. NOAA, JPL U.K., Switzerland Denmark Canada
SAM-II	Daily aerosol profiles Seasonal and annual contour maps and atmospheric cross sections	Aerosol backscatter profiles Optical Properties of stratospheric aerosols	Atmospheric sinks Earth radiation budget studies Aerosol injection dynamics	LaRC, U of Wyo. NCAR, SRI, U of Ariz. NOAA
LIMS	Daily atmosphere profile Daily, monthly and seasonal contour maps and atmospheric cross sections	Gas concentrations and temperature profiles in the stratosphere	Atmospheric pollution monitoring Photo-chemical studies Atmospheric gas dynamics Climatology	LaRC, NCAR, NOAA Drexel, U of Mich U of Wash, JPL UK France
SAMS	Daily atmospheric profile Daily, monthly, and seasonal contour maps and atmospheric cross sections	Gas concentrations and temperature profiles in the stratosphere and mesosphere	Atmospheric pollution monitoring Photo-chemical studies Atmospheric gas dynamics Climatology Wind dynamics	Oxford GSFC LaRC Drexel NCAR
SBUV/TOMS	Daily profiles of O_3 Daily, monthly and seasonal contour maps Solar spectra Zonal O_3 statistics	O_3 profiles Total atmospheric O_3 Solar irradiances Terrestrial radiances	O_3 dynamics/modelling Climatology and meteorology O_3 solar relationships	GSFC, NOAA, MIT, CDC, U of Fla. NSF, LARC Lockheed, Oxford Cal Tech Canada
CZCS	2-minute images	Temperature Spectral radiances Chlorophyll Sediment	Geodynamics of coastal regions Chemical and thermal pollution studies Fishery resources Deep ocean monitoring Oil spill monitoring	GSFC, NOAA, U of Cal (Davis) U of Fla. AMES Tex A&M EURASEP
THIR	Daily montages of temperature	Surface temperature Cloud top temperature	Effects of cloudiness or other Nimbus-G instruments data	All sensors

Table 2. NIMBUS-7 data products and users.

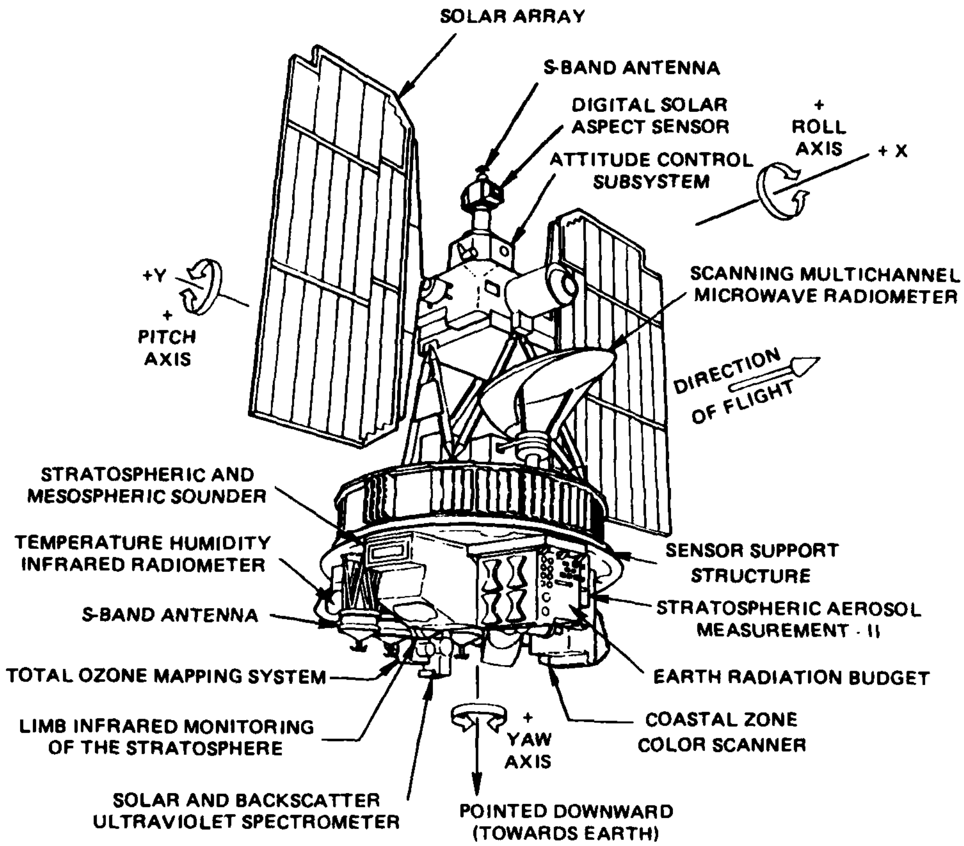

Figure 2. NIMBUS-7 spacecraft.

3. Provide additional and continued earth surface sensing capability related to:
   a. Cloud cover
   b. Cloud-land-ocean temperature mapping
   c. Earth IR radiation measurements

The spacecraft operated in a near polar orbit at an altitude of 955 kms, with an orbital period of roughly 104 minutes. The longitudinal separation (at the equator) for successive orbits was 26° or approximately 160 nms. The system operating goal was one year in orbit.

The NIMBUS-7 spacecraft weighs 2123 pounds and has a configuration similar to an ocean buoy. It is 10 feet tall, 5 feet in diameter at the base, and 13 feet wide with the solar paddles fully extended. The sensor mount that forms the satellite base houses the electronics equipment and battery modules. The lower surface of the torus provides mounting space for sensors and antennas. A boxbeam structure mounted within the center of the torus provides support for the larger sensor experiments. The control housing unit is located on top of the spacecraft and above this unit are the sun sensors, horizon scanners and a command antenna.

The spacecraft power subsystem consists of solar arrays, nickel-cadmium batteries, charge and discharge regulators and voltage regulators to operate all spacecraft support subsystems and to provide maximum power for the instrument payload.

The orbit average regulated power provided by the observatory power subsystem is approximately 300 watts, of which 123 watts are allocated to the spacecraft subsystems. If all the instruments were on full-time, the power requirements would exceed the available supply. Because of this power limitation, the subsystems will operate for approximately the percentage of time given in Table 3. Only the temperature and humidity IR radiometer (THIR) is scheduled to operate on a full-time basis. This schedule is in accordance with the specific objectives of the NIMBUS project.

Instrument	Power Requirements, watts	Operational Mode, %
CZCS	11.4	30
ERB	36.3	80
LIMS	24.5	80
SAM II	0.8	8
SAMS	23.0	80
SBUV/TOMS	20.0	80
SMMR	61.6	50
THIR	8.5	100
Subsystem Total	186.1	
Basic Spacecraft	123.6	
Observatory Total	309.7	

Table 3. Instrument power requirements for the percentage of operational time allotted each sensor.

The NIMBUS-7 communications and data handling subsystem (CDHS) is composed of the S-band communications system and tape recorder subsystem and handles all spacecraft information flow. The S-band communication system includes the S-band command and telemetry system, the data processing system (DPS) and the command clock. The S-band command and telemetry system consists of two S-band transponders, a command and data interface unit (CDIU), four earth-view antennas, a sky-view antenna and two S-band transmitters (2211 MHz). Commands are transmitted to the observatory by pulse code modulation (PCM), phase-shift keying (PSK)/frequency modulation (FM) and phase modulation (PM) of the assigned 2093.5 MHz S-band uplink carrier. Stored command capability provides for command execution at predetermined times.

Table 4 lists the NIMBUS-7 contractors.

Company	Contribution
Prime Contractor:	
General Electric Co. Space Systems Space Division Valley Force, Pennsylvania	• Spacecraft structure and antennas • Separation and unfold subsystem • Thermal control subsystem • Electrical distribution harness • Electro-mechanical components • Ground support equipment • Attitude control system components • Spacecraft integration and test • Spacecraft subcontracts management
Contributing Contractors:	
Gulton Industries Albuquerque, New Mexico	• Earth radiation budget
Ball Bros. Boulder, Colorado	• Coastal zone color scanner
Beckman Instruments Fullerton, California	• Solar backscatter ultra-violet energy and total ozone mapping spectrometer
Bendix Corporation Teterboro, New Jersey	• Pitch and yaw momentum wheels
California Computer Products Anaheim, California	• Command/clock subsystems • Interface switching modules
Control Data Corporation Philadelphia, Pennsylvania	• Ground station computer
Fairchild Hiller Germantown, Maryland	• Attitude control system structure • Attitude control system thermal control louvers
Honeywell Boston, Massachusetts	• LIMB infrared monitoring of the stratosphere experiment
Ithaco Ithaca, New York	• Magnetic moment compensating assembly • Roll reaction wheel scanner/signal processor • Control logic box
Jet Propulsion Laboratories Pasadena, California	• Scanning multichannel microwave radiometer experiment
Kearfott Clifton, New Jersey	• Rate measuring package gyro (ball bearing)
Lear Siegler, Inc. Anaheim, California	• Ground station computer
Ludwig Honold Philadelphia, Pennsylvania	• Flight adapter structure
Motorola, Inc. Scottsdale, Arizona	• S-band transponder

Table 4. NIMBUS-7 contractors.

Company	Contribution
Northrop Corporation Electronics Division Norwood, Massachusetts	• Yaw rate gyro • Rate measuring package gyro (gas bearing)
Oxford University, U.K. and Hawkee-Siddley Stevenage, Herts SG1 2AS	• Stratospheric and mesospheric sounder
Parsons Stockton, California	• Solar array assembly
Radio Corporation of America Communications System Div. Camden, New Jersey	• Tape recorder
Radio Corporation of America Astro Electronics Division Princeton, New Jersey	• Power subsystem (regulator, storage modules)
Rutherford Laboratory Chilton, Didcot Berkshire, England and Elliott Automation Frimley, Camberly Surrey, England	• Pressure modulation radiometer experiment
Santa Barbara Research Center Santa Barbara, California	• Temperature humidity infrared radiometer
Spectrolab, Inc. Sylmar, California	• Solar array substrates
Sperry Gyroscope Great Neck, L.I., New York	• Rate measuring package (ball and gas bearing gyros)
Teledyne Los Angeles, California	• S-band transmitters
TRW Redondo Beach, California	• Attitude control pneumatics Solar array drives
University of Wyoming Laramie, Wyoming	• Stratospheric aerosol measurement II

Table 4. (Continued)

2.2 LANDSAT

The LANDSAT program evolved from the earlier ERTS (Earth Resources Technology Satellite) program. The LANDSAT spacecraft and its orbital patterns are quite similar to the previously described NIMBUS-7. The LANDSAT program is managed by NASA's Office of Space and Terrestrial Applications. Actual day-to-day project management is centered at NASA's Goddard Space Flight Center (GSFC). The prime contractor is the GE Space Division. The primary sensor used in LANDSAT-1, -2 and -3 is the MSS (multispectral scanner), which was developed by Santa Barbara Research Corporation of Hughes Aircraft Company (Goleta, California).

A follow-on effort will see the launch of "quasi-operational" LANDSAT D (probably mid-1982) and LANDSAT D′ (probably mid-1983). LANDSAT D′ will probably carry the Thematic Mapper (TM) which also was developed by Hughes.

The primary goal of LANDSAT is to provide good spectral imaging of surface terrain and accompanying growing vegetation throughout the world. These data are obtained using the MSS. A limited amount of additional "image" data has been obtained in the visible, using the TV camera RBV (Return Beam Vidicon).

A concise history (and projection) of the LANDSAT program status is given in Table 5, while Table 6 provides a summary of LANDSAT operations up to September 1980.

Primary governmental users of the data generated by the MSS are the Department of Agriculture (for crop and forestry assessments) and the U.S. Geological Survey (for determining fault lines and rock characteristics which are useful in petroleum and mineral exploration).

When a fully operational status is obtained by LANDSAT's D and D′, the day-to-day operations of the system will be taken over by NOAA/NESS.

Satellite	Launch	Status
LANDSAT-1	July 23, 1972	Ceased data collection January 10, 1978
LANDSAT-2	January 22, 1975	Ceased data collection November 5, 1979
LANDSAT-3	March 5, 1978	In operation
LANDSAT D	Planned for Summer 1982	Under development
LANDSAT D′	Available for launch 6 months after D	Approved

Table 5. LANDSAT program status.

	U.S.		Foreign	
Scenes Acquired (September 1980)	MSS	RBV	MSS	RBV
LANDSAT-1*	149,640	1,546	122,146	144
LANDSAT-2*	151,955	2,289	231,987	542
LANDSAT-3*	49,858	16,754	96,240	56,542

All digital data MSS production initiated 2/1/79

Backlog 3/2/80	5,659 scenes
Current acquisition rate	345 scenes/week (average past 4 weeks)
Current processing rate	621 scenes/week (average past 4 weeks)
Backlog eliminated	8/15/80 date (at present acquisition rate)
Current turnaround time (GSFC)	80% complete within 5 days (February sample)

All digital RBV production 3/31/80

*LANDSAT-1 (Launched 23 July 1972, Shut down 16 January 1978)
LANDSAT-2 (Launched 22 January 1975)
LANDSAT-3 (Launched 15 March 1978)

Table 6. LANDSAT operations – summary.

2.3 TIROS-N/NOAA-A

TIROS-N and its twin NOAA-A are operational weather satellites, managed by NOAA/NESS. These satellites operate in sun-synchronous, near polar, orbits to provide cloud cover, surface, temperature, atmospheric temperature and humidity profiles, etc. These satellites were designed and built by RCA Astro-Electronics in Princeton, New Jersey. NASA funded the development and launch of TIROS-N; NOAA provided the funds to NASA for the procurement and launch of NOAA-A (sometimes designated NOAA-6). Each satellite cost approximately $20M.

The satellites were launched from NASA's Western Test Range, using ATLAS-F boosters. Each satellite has an estimated design operating life of roughly two years.

Figure 3 depicts TIROS-N. The TIROS-N spacecraft is 12 feet long and six feet wide. Its solar panels have a collecting area of approximately 125 square feet.

Table 7 lists the basic characteristics of TIROS-N/NOAA-A.

Four primary spacecraft instrument systems are aboard these satellites: the Advanced Very High Resolution Radiometer (AVHRR), the TIROS Operational Vertical Sounder (TOVS), the Data Collection System (DCS) and the Space Environment Monitor (SEM).

The AVHRR will provide image data for real-time transmission to both Automatic Picture Transmission (APT) and High Resolution Picture Transmission (HRPT) users and for storage on the spacecraft tape recorders for later playback.

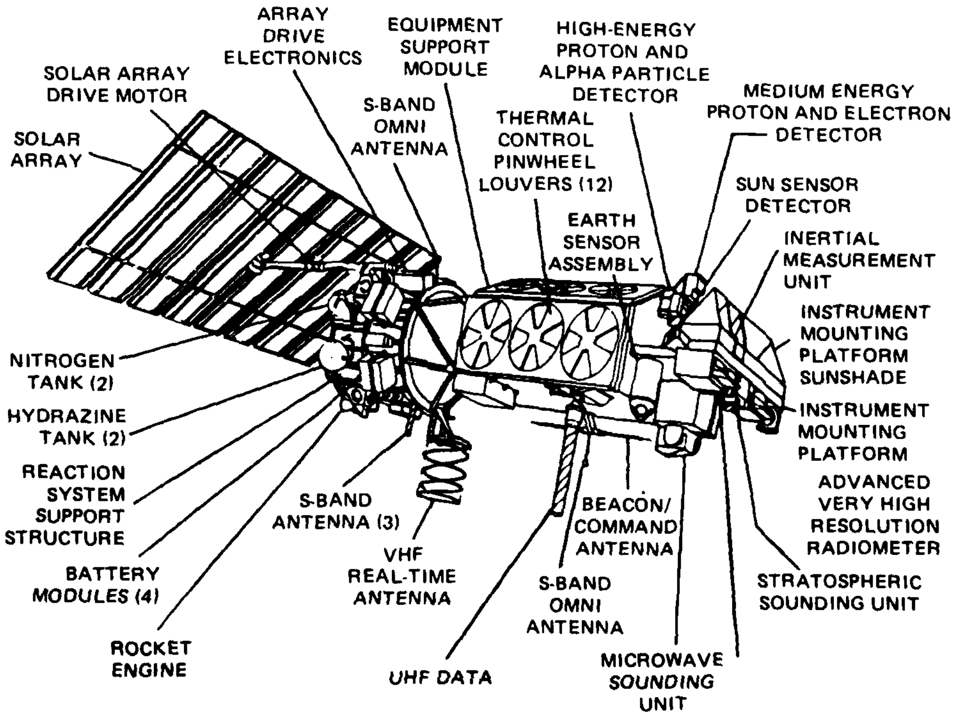

Figure 3. TIROS-N spacecraft.

Spacecraft	:	Total weight (includes expendables)	1421 kg (3127 lb)
Payload	:	Weight including tape recorders	194 kg (427 lb)
	:	Reserved for growth	36.4 kg (80 lb)
Instrument Complement	:	Advanced Very High Resolution Radiometer (AVHRR) High Resolution Infrared Radiation Sounder (HIRS/2) Stratospheric Sounder Unit (SSU) Microwave Sounder Unit (MSU) Data Collection System-ARGOS (DCS) Space Environment Monitor (SEM)	
Spacecraft Size	:	3.71 meters in length (146 in.) 1.88 meters in diameter (74 in.)	
Solar Array	:	2.37 m X 4.91 m : 11.6 sq m (7.8 ft X 16.1 ft : 125 sq ft) 420 watts, end of life, at worst solar angle	
Power Requirement	:	Full operation -- 330 watts Reserved for growth -- 90 watts	
Attitude Control System	:	0.2° all axes 0.14° determination	
Communications			
Command Link	:	148.56 MHz	
Beacon	:	136.77; 137.77 MHz	
S-Band	:	1698; 1702.5; 1707 MHz	
APT	:	137.50; 137.62 MHz	
DCS (uplink)	:	401.65 MHz	
Data Processing	:	All digital (APT; analog)	
Polar Orbit	:	TIROS 833; NOAA-A 870 km nominal altitudes	
Launch Vehicle	:	Atlas E/F	
Lifetime	:	2 years planned	

Table 7. TIROS-N/NOAA-A summary sheet.

2.4 Geostationary Operational Environmental Satellite (GOES)

The GOES (Geostationary Operational Environmental Satellite) is an operational weather satellite, managed by NOAA/NESS. The technological developments and launches were provided to NOAA by NASA GSFC. The GOES satellites are the source of the nightly satellite weather pictures on TV. The GOES satellites are in geostationary orbits, approximately 19,600 nm above the equator. The "Eastern Bird" (GOES-3) is located above the equator at 75°W longitude and the "Western Bird" (GOES-4) is at 135°W longitude.

To date there have been four successful launches of GOES spacecraft, as shown in Table 8. Each of these spacecraft was launched from NASA's Eastern Test Range (Cape Canaveral, Florida).

Spacecraft	Launch Year	Manufacturer
GOES-1	1975	Ford Aerospace and Communications Corporation, Palo Alto, California
GOES-2	1977	Ford Aerospace and Communications Corporation, Palo Alto, California
GOES-3	1978	Ford Aerospace and Communications Corporation, Palo Alto, California
GOES-4	1980	Hughes Aircraft Company, Space and Communications Group, Fullerton, California

Table 8. GOES spacecraft.

Figure 4 depicts GOES-4. The spacecraft was launched using a DELTA 3914 launch vehicle. GOES-4 has an estimated operating design life of roughly seven years; Table 9 lists its characteristics.

The primary sensor of major interest aboard GOES-4 is VAS (Visible and IR Spin Scan Radiometer and Atmospheric Sounder). This sensor provides cloud and temperature imaging in terms of visible and IR spectra. The combination GOES-3 and GOES-4 provides cloud cover data in the Western Hemisphere between latitudes 60°N and 60°S. Cloud cover data closer to the poles is provided by the TIROS-N/NOAA-A system.

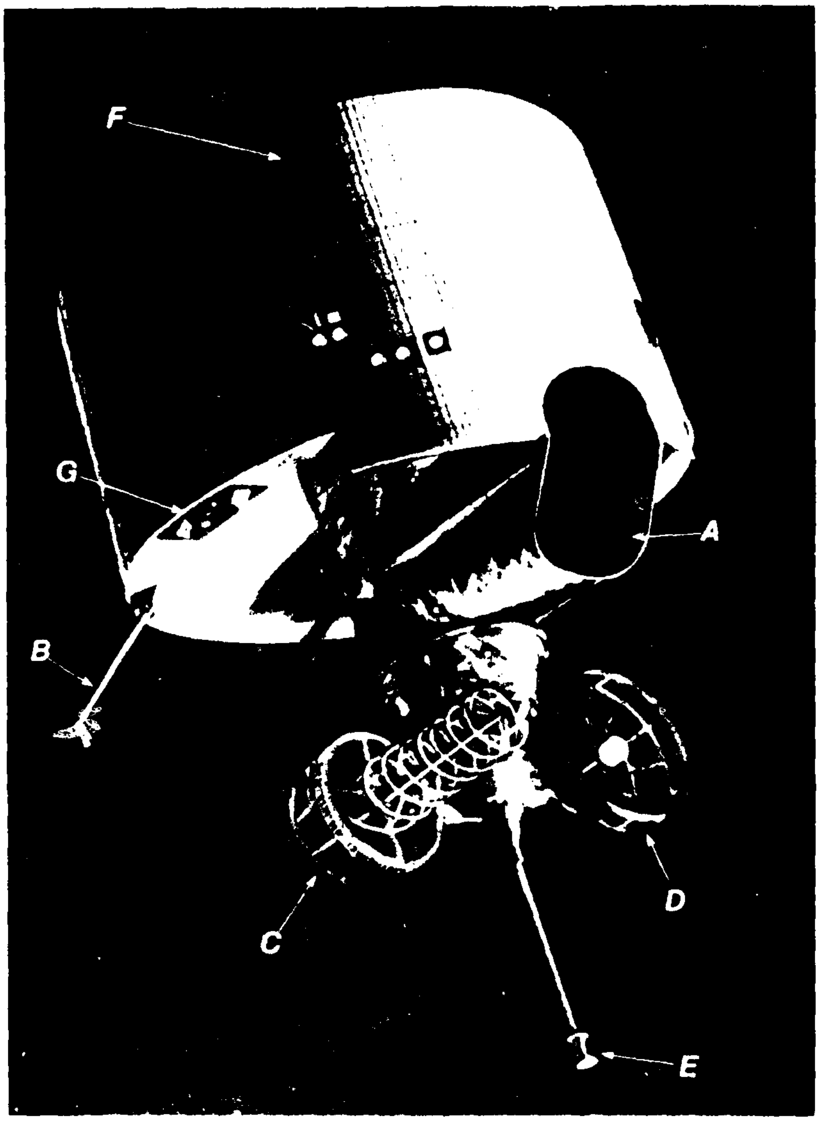
F
G
A
B
C
D
E

Launch Vehicle	Delta 3914
Spacecraft Mass, lb	
Launch (separated spacecraft)	1841.0
On station beginning of life	874.0
On station end of life (dry weight)	762.0
Spacecraft Dimensions, in.	
Length along Z-axis	174.3 (with adapter) 138.7 (without adapter)
Diameter	84.5
Apogee Motor	Thiokol TE-M 616 derivative
Communications	
Coverage at S-band Coverage at UHF	Visible earth-western hemisphere
Frequencies	

Multifunction Repeater	Multifunction/VAS	WEFAX	Trilateration
Receive, MHz	2029.1 (S VAS)	2033.0	2026.0 2030.2 2032.2
Transmit, MHz	1681.6 (VAS) 1687.1 (S VAS)	1691.0	1684.0 1688.2 1690.2

Frequencies	MFR	DCPI	DCPR	CDA TM	STDN TM	STDN RNG	STDN/CDA CMD
Receive, MHz	See	2034.925	401.9	–	–	2034.2	2034.2
Transmit, MHz	above	468.850	1694.5	1694.0	2214.0	2209.086	-
EIRP, dBM	56.[illegible]	46.2	35.6	33.4	26.6	13.9	–
Margins, dB*	3.3	9.1	10.0	6.9	7.8	11.4	...
G/T, dB/°K	-17.6	-17.6	-18.5	–	–	-36.9	-36.9
Margins, dB	7.4	7.4	6.5	–	–	3.1	3.1
Bandwidth, MHz	8.2/20	0.2	0.4	0.1	0.1	1.0	0.08

Antennas	
S-band (high gain)	Parabolic, linear (vertical) polarization – 18.2/18.1 dB peak gain transmit/receive
UHF	Helix, RHCP – 11.7/9.4 dB peak gain transmit/receive
S-band (T&C)	Bicone-linear (vertical) polarization – 1.0/3.0 dB peak gain transmit/receive
Antenna Pointing, deg	
East-west	⩽±0.5 (sun reference) ⩽±0.75 (earth reference)
Attitude Control and Stationkeeping	
On-orbit spin to transverse inertia ratio (EOL)	$\pm 1.13\ I_{ZZ}/I_{TEFF}$
On-orbit spin stabilized	On-orbit spin rate: 100 rpm
Attitude	Axial jet control to ±0.2°
N-S stationkeeping	Axial jet control to ± 1.0°
E-W stationkeeping	Adjacent pair of radial jets for control to ±0.5°
Spin rate	Moment pair of radial jets for control to ±5 rpm
Transfer Orbit Spin Stabilized	
Transfer orbit	Spin rate 55 rpm
Attitude control	Axial jet control with automatic nutation control. Time constant < 10 sec
Active nutation control moment	3.7 ft-lb
Predicted stability margin	>1500:1 at threshold (0.2°) (T dedamp/T damp)
Fuel usage	1.0 lb (9 orbits)
Attitude Determination	
Sensors	Earth and sun
Accuracy	<±0.1° (on orbit); ±0.5° (transfer orbit)

Table 9. GOES-4 characteristics.

3.0 SENSORS

The non-DoD satellite-borne sensor systems of potential interest to the Navy's ocean surveillance community can be divided into two general categories: (1) those operating in the visible and IR portions of the electromagnetic spectrum and (2) those in the microwave region.

Sensors operating in the visible and IR domain to be discussed include:

- MSS (multispectral scanner)
- CZCS (coastal zone color scanner)
- AVHRR (advanced very high resolution radiometer)
- VAS (visible and IR spin scan radiometer and atmospheric sounder)
- TM (thematic mapper)
- SMIRR (shuttle multiband visible/IR radiometer)
- MLA (multispectral linear array).

Sensors operating in the microwave domain to be discussed include:

- SAR (synthetic aperture radar)
- MS (microwave scatterometer)
- SMMR (scanning multichannel microwave radiometer).

All of the preceding sensor systems are passive with the exception of SAR. The MSS, CZCS, AVHRR, VAS, SAR and SMMR have all been operated successfully aboard various spacecraft. The TM and SMIRR have undergone limited engineering tests on the ground. The MLA is just entering the conceptual design phase and a "flyable" unit will not be ready until 1989.

3.1 VISIBLE/IR SENSORS

The sensors to be discussed are passive devices, operating in the visible and IR portion of the electromagnetic spectrum. Most utilize reflected solar energy and thus are limited to daylight operations.

3.1.1 COASTAL ZONE COLOR SCANNER (CZCS)

The CZCS has been successfully aboard NIMBUS-7. It was used primarily to determine the nature of suspended particulate matter and chlorophyll in coastal and open ocean waters.

The CZCS is a conventional multi-channel scanning radiometer utilizing a rotating plane mirror at a 45° angle to the optic axis of a Cassegrain telescope. The rotating mirror scans 360°; however, only ±40° of data centered on the spacecraft nadir are collected for ocean color measurements. During the rest of the scan, the instrument acquires a view of deep space and of internal instrument sources for calibration of the various channels. The radiation collected by the telescope is divided into two portions by a dichroic beam splitter. One portion is transmitted to a field stop that is also the entrance aperture of a small polychromator. The radiant energy entering the polychromator is dispersed and reimaged in five wavelengths on five silicon detectors in the focal plane of the polychromator. The portion of the beam reflected off of the dichroic mirror is directed to a cooled mercury cadmium telluride detector sensing in the 10.5 μm to 12.5 μm region. The CZCS utilizes a radiative cooler that cools the mercury cadmium telluride detector to approximately 120° Kelvin during spacecraft flight.

The CZCS scanning system is depicted in Figure 5 while the CZCS device is depicted in Figure 6 and the CZCS optical arrangement is shown in Figure 7. Performance parameters are listed in Table 10 and the CZCS spectral bands/channels in Table 11.

Channels 1-5 depend on reflected sunlight and, therefore, are operable during daylight hours (local time). Channel 6 depends upon thermally radiated energy at the ocean surface and is operable day and night. Radiation detectors for channels 1-5 consist of silicon photodiodes while channel 6 employs a radiatively cooled (HgCd) Te photoconductor. The six channels of digital radiometric data are tape recorded and later transmitted to ground stations using 800 kbps biphase telemetry at S-band.

3.1.2 MULTISPECTRAL SCANNER (MSS)

The characteristics of the Hughes MSS are summarized in Figure 8. The incoming light is dispersed from a reflecting grating. The MSS utilizes spectral bands in the visible, centered at 0.55 μm, and 0.65 μm and two bands in the near IR, centered at 0.75 μm and 0.95 μm. The detectors are silicon photodiodes.

The MSS depends on the presence of reflected sunlight and, therefore, is operable only during daylight hours (local time). The scan is obtained mechanically by vibrating a mirror transverse to the spacecraft's motion.

The MSS has been flown successfully aboard LANDSAT-1, -2 and -3 and is scheduled for use aboard LANDSAT-D and -D'.

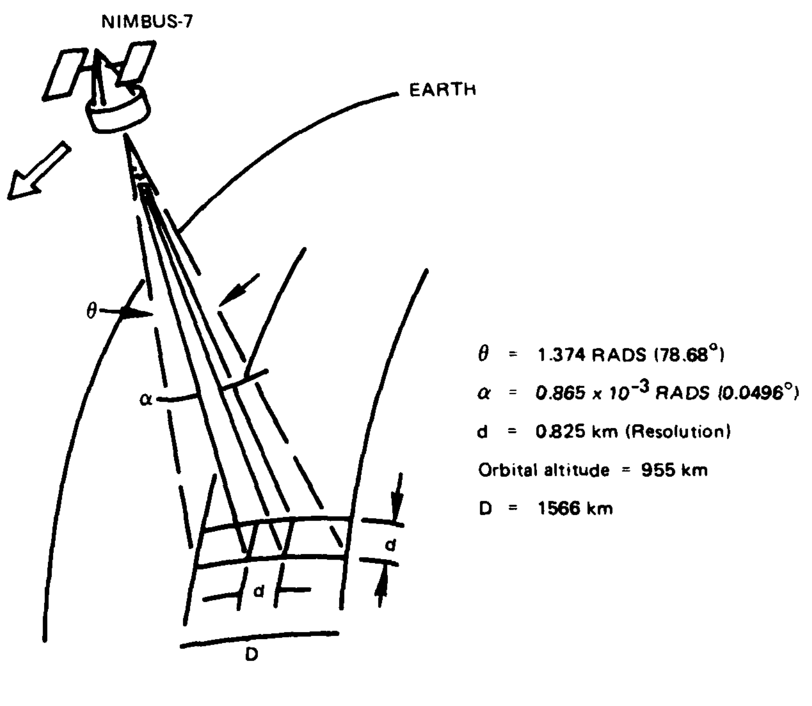

Figure 5. CZCS scanning arrangement and parameters.

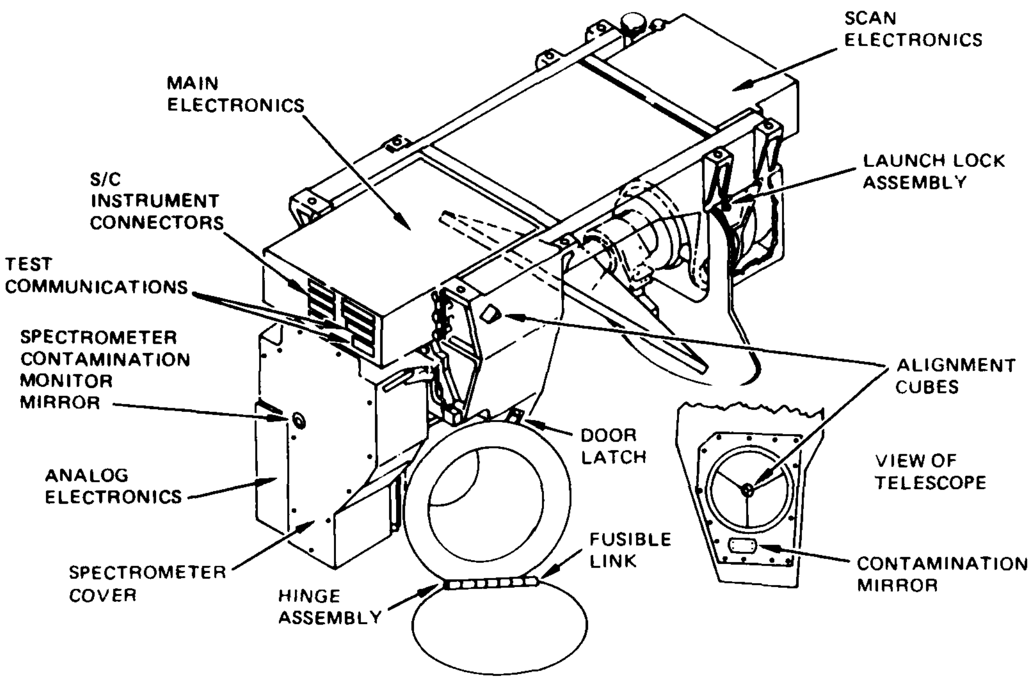

Figure 6. The CZCS.

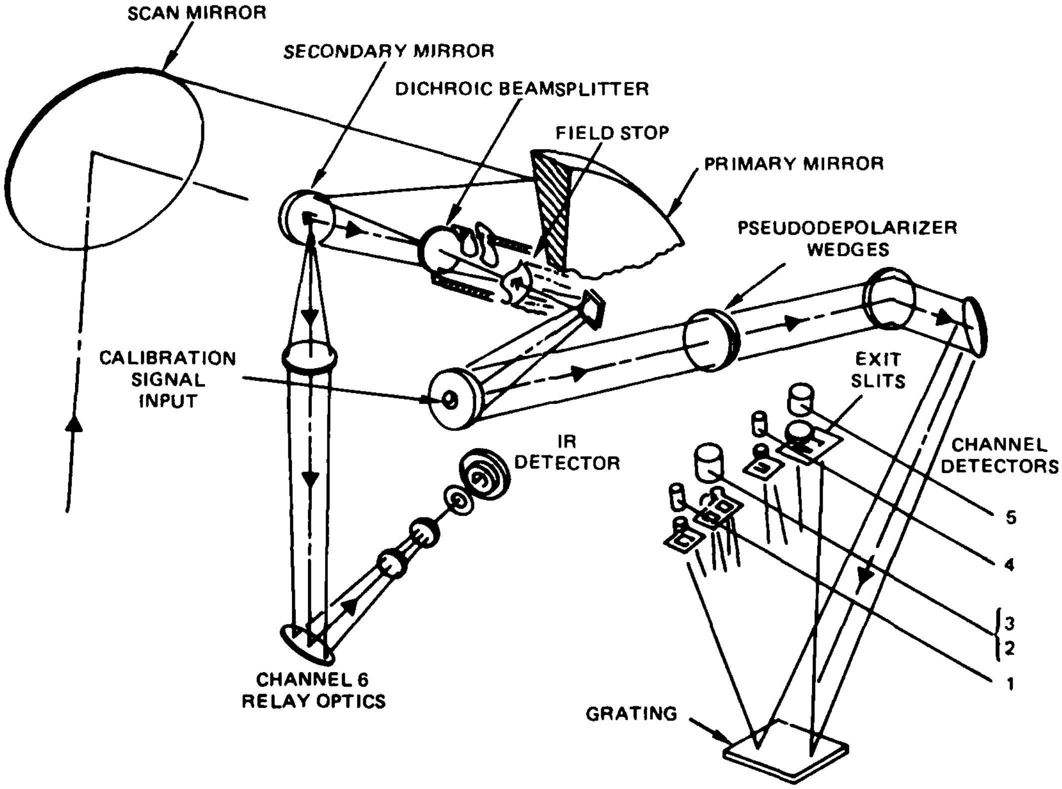

Figure 7. CZCS optics.

Performance Parameters	Channels 1	2	3	4	5	6
Scientific observation	Chlorophyll absorption	Chylorophyll correlation	Yellow stuff	Chylorophyll absorption	Surface vegetation	Surface temperature
Center wavelength λ micrometers	0.443 (blue)	0.520 (green)	0.550 (yellow)	0.670 (red)	0.750 (far red)	11.5 (infrared)
Spectral bandwidth Δλ micrometers	0.433 – 0.453	0.510 – 0.530	0.540 – 0.560	0.660 – 0.680	0.700 – 0.800	10.5 – 12.5
Instantaneous field of view – Spatial resolution	0.865 X 0.865 Milliradians (0.825 X 0.825 km at sea level)					
Co-registration at NADIR	< 0.15 Milliradians					
Accuracy of viewing position information at NADIR	< 2.0 Milliradians					
Signal-to-noise ratio (min.) at Radiance input N < (mW/cm²·STER·μm)	> 150 at 5.41	> 140 at 3.50	> 125 at 2.86	> 100 at 1.34	> 100 at 10.8	NETD of 0.220°K at 270°K
Consecutive scan overlap	25%					
Modulation transfer function (MFT)	1 at 150 km target size, 0.35 min. at 0.825 km target size					

Table 10. CZCS performance parameters.

Channel No.	Channel Response, μm	Signal-To-Noise Ratio at Specified Radiance	NEΔT at Specified Temperature
1	.433 – .453	218 @ 5.41 mW/cm²·STER·μm	
2	.510 – .530	209 @ 3.50	
3	.540 – .560	196 @ 2.86	
4	.660 – .680	119 @ 1.34	
5	.700 – .800	244 @ 10.8	
6	10.5 – 12.5		0.15K @ 270K

Table 11. CZCS spectral bands/channel.

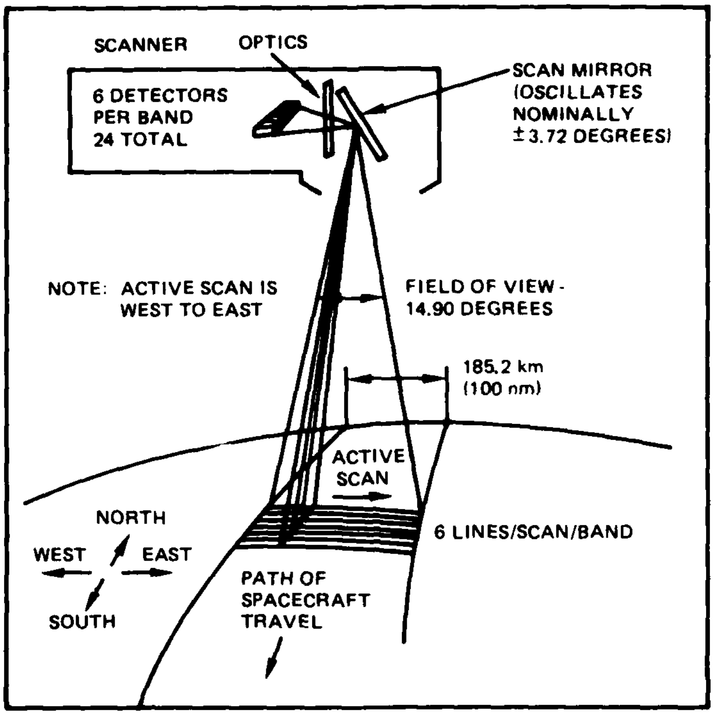

- WEIGHT: 144 POUNDS
- SIZE: SCANNER – 24 IN X 35 IN X 16 IN
  MULTIPLEXER – 6 IN X 4 IN X 7 IN
- POWER: 75 WATTS MAX. OPERATING
- DATA RATE: 15.06 MBPS AND INCLUDES
  - VIDEO DATA
  - TIME CODE (EVERY OTHER SCAN)
- SPECTRAL BANDS

  BAND 1: 0.5 TO 0.6 MICROMETERS
  BAND 2: 0.6 TO 0.7 MICROMETERS
  BAND 3: 0.7 TO 0.8 MICROMETERS
  BAND 4: 0.8 TO 1.1 MICROMETERS
- INSTANTANEOUS FIELD OF VIEW: 83 METERS

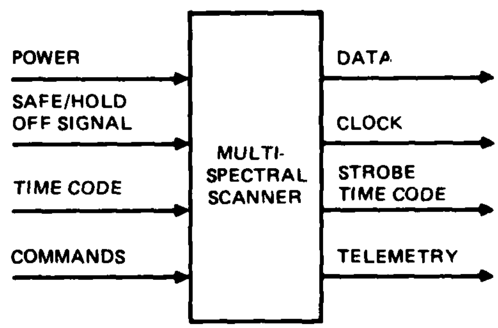

Figure 8. Hughes MSS (aboard LANDSAT-1, -2, -3).

3.1.3 ADVANCED VERY HIGH RESOLUTION RADIOMETER (AVHRR)

The AVHRR is an IR sensing instrument aboard TIROS-N that is used remotely to determine surface temperature. A scanning radiometer, its characteristics are listed in Table 12.

The detectors for each of the five spectral channels are squares, 0.254 cm on a side. The instantaneous field of view (IFOV) which they see 1.3 X 1.3 mrad corresponds to a ground resolution of 1.1 km at nadir. Channels 3 and 5 are used to provide both day and night sea-surface temperatures. Video image data are transmitted at 120 lines per minute using outputs from the AVHRR.

The AVHRR optical system consists of an 8-inch aperture telescope combined with a diffraction grating to generate the five spectral bands. A scanning mirror rotates at 360 rpm to produce a cross-track scan.

Characteristics	Channels				
	1	2	3	4	5
Spectral range (micrometers)	0.58 to 0.68	0.725 to 1.0	10.3 to 11.3	3.55 to 3.93	11.5 to 12.5
Detector	Silicon	Silicon	(HgCd) Te	InSb	(HgCd) Te
Resolution (km)	1.1	1.1	1.1	1.1	1.1
Instantaneous field of view (IFOV) (milliradians)	1.3 sq.	1.3 sq.	1.3 sq.	1.3 sq.	1.3 sq.
Signal-to-noise ratio @ 0.5 albedo	> 3:1	> 3:1	-	-	-
Noise-equivalent temperature difference @ 300°K		–	0.12 @ 300°K	0.12 @ 300°K	0.12 @ 300°K
Modulation transfer function (one IFOV/single bar)	0.30	0.30	0.30	0.30	0.30

Optics – 8-inch diameter afocal Cassegrainian telescope

Scanner – 360-rpm hysteresis synchronous motor with beryllium scan mirror

Cooler – Two-stage radiant cooler, infrared detectors controlled at 105° or 107°K

Data output – 10-bit binary, simultaneous sampling at 40-kHz rate

Table 12. AVHRR characteristics.

3.1.4 VISIBLE AND IR SPIN SCAN RADIOMETER AND ATMOSPHERIC SOUNDER (VAS)

VAS operates aboard GOES-4 as a visible and IR scan radiometer. The scanning process is produced by the rotation of the GOES-4 spacecraft. The operation of VAS is depicted in Figure 9.

Visible spectral data (0.55 - 0.75 μm) are detected using an array of eight photomultiplier tubes; each tube views an eighth of the scan width.

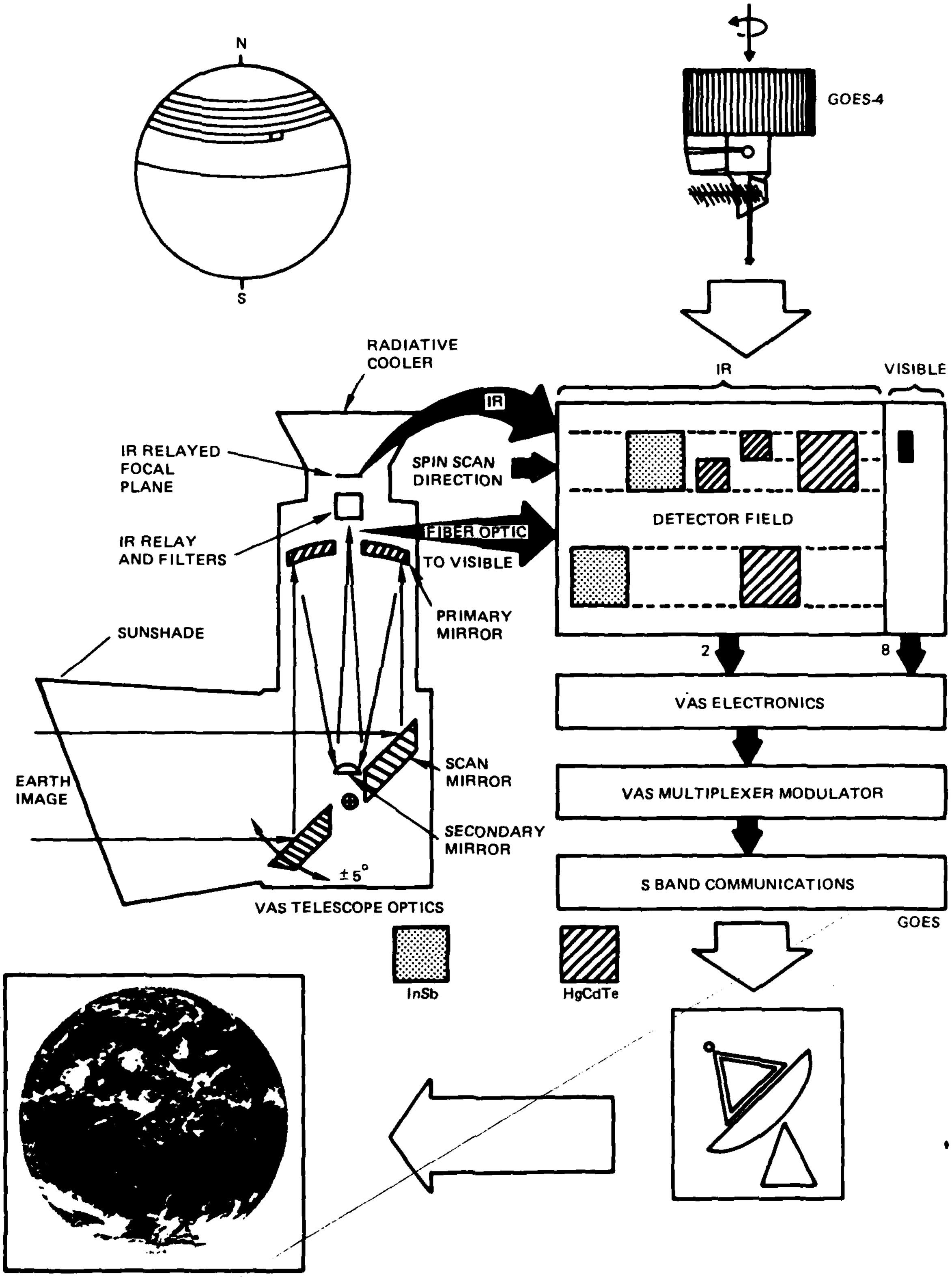

Figure 9. VAS system.

The IR spectrum (from narrow band filters) is collected in 12 bands, as listed in Table 13.

The VAS optical system utilizes a Ritchey-Chretien type telescope (similar to Cassegrain optics, except for surface contours which produce a larger field of view at the focal plane). Two focal planes are used in VAS. Visible spectrum signals are obtained at the principal focus. An optical fiber for each of the eight instantaneous fields of view defines the field to be imaged (24 X 25 μrad) and conducts the corresponding light images to each of the eight photomultiplier tubes. The IR field of view is 192 μrad.

The spatial resolution at the earth's surface in the visible channel is approximately 1 km. The resolution in the IR channels is 8 km. Detailed characteristics of VAS are summarized in Table 14.

3.1.5 THERMAL MAPPER (TM)

The TM is a multispectral scanning radiometer covering spectral bands in the visible and IR. It is scheduled to be flown aboard LANDSAT D or D′ to perform an "earth resources" mapping function. An engineering model, tested in the laboratory, uses a rotating mirror for scanning. Figure 10 depicts the operation of the system.

Figure 11 summarizes the characteristics of TM; while Figure 12 is a cross-sectional view of TM. The significant TM parameters are summarized in Table 15.

TM has two focal planes on which ground images are focused. The prime focal plane assembly has 16 detectors in four spectral bands and the secondary focal plane (which is cooled) has three bands with 20 detectors. The optical configuration is depicted in Figure 13. Spectral responses of the seven spectral bands are listed in Table 16.

				Remarks		S/N Improvement Requirements		
Spectral Band	Atmospheric Pressure, mb	λ, μm	Δν, cm^{-1}	Band	Detector Type	NEN/ IGFOV*	Sounding NEN*	Spin Budget
1	65	14.73	10	CO_2	HgCdTe	10.390	0.25	6
2	100	14.48	16	CO_2	HgCdTe	3.490	0.25	14
3	325	14.25	16	CO_2	HgCdTe	3.000	0.25	11
4	450	14.01	20	CO_2	HgCdTe	2.200	0.25	7
5	Surface	13.33	20	CO_2	HgCdTe	2.080	0.25	7
6	700	4.525	45	CO_2	InSb	0.063	0.004	35
7	Surface	12.66	20	H_2O	HgCdTe	1.930	0.25	7
8	Surface	11.17	140	Window	HgCdTe	0.296	0.25	1
9	375	7.261	40	H_2O	HgCdTe	1.770	0.15	16
10	330	6.725	150	H_2O	HgCdTe	0.482	0.10	3
11	280	4.444	40	CO_2	InSb	0.073	0.004	46
12	Surface	3.945	140	Window	InSb	0.022	0.004	4

*Ergs/cm^2-sec-sr-cm^1

Table 13. VAS IR spectral bands.

Size	
Length	~ 1.5 m
Radial dimension	~ 0.65 m
Weight	
Scanner	64.3 kg
Electronics module	10.5 kg
Structural material	Beryllium (structure and mirrors)
Optics	Ritchey-Chretien system 40.64 cm dia primary mirror Focal length 292.1 cm Optically flat scan mirror
Detectors	
Visible spectrum	8 photomultiplier tubes coupled to focal plane by optical fibers *which define IGFOV: 21 X 25 μrad*
Infrared spectrum	Solid state detectors cooled to 95°K 2 HgCdTe; IGFOV: 192 μrad 2 HgCdTe; IGFOV: 384 μrad 2 InSb; IGFOV: 384 μrad
Spectral bands	By filters inserted in IR optical path; 12 filters selectable from rotating wheel
Radiative cooler	Servoed operating temperature ~ 95°K Heat rejection capacity ~ 16 mw Minimum temperature ~ 82°K
In-orbit calibration	Radiometric IR: Temperature monitored blackbody, cyclically reflected into optical axis Visible: Optical aperture providing sun signal of 50% earth albedo Electronic IR and Visible: Stairstep voltage into amplifier chain
Onboard programmer	Reprogrammable by command link Selects and controls scan sector size and center position Controls filter wheel and selects transmitting detector pair

Table 14. VAS characteristics.

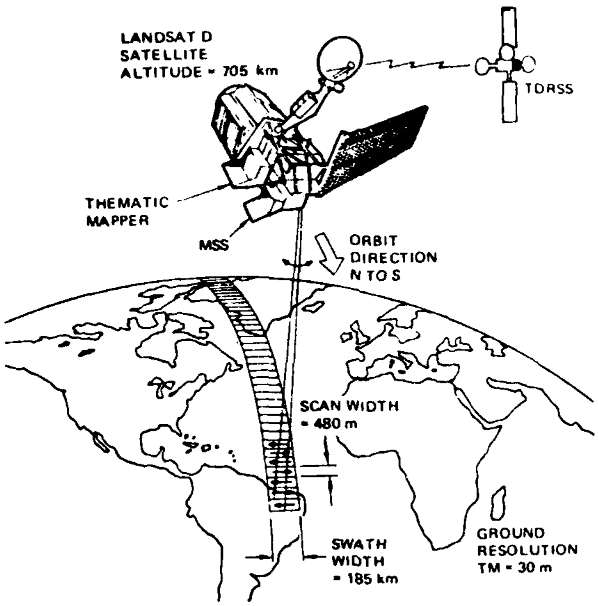

Figure 10. TM operations on LANDSAT D′.

- WEIGHT: 570 POUNDS
- SIZE 76 IN X 43 IN X 28 IN
- POWER: 300 WATTS OPERATING
  75 WATTS STANDBY
- DATA RATE: 34.0 MBPS AND INCLUDES
  - VIDEO DATA
  - TIME CODE
  - FLIGHT SEGMENT TELEMETRY
- SPECTRAL BANDS:
  BAND 1: 0.45 – 0.52 MICROMETERS
  BAND 2: 0.52 – 0.60 MICROMETERS
  BAND 3: 0.63 – 0.69 MICROMETERS
  BAND 4: 0.76 – 0.90 MICROMETERS
  BAND 5: 1.55 – 1.75 MICROMETERS
  BAND 6: 10.4 – 12.5 MICROMETERS
  BAND 7: 2.08 – 2.35 MICROMETERS
- INSTANTANEOUS FIELD OF VIEW:
  BAND 6 120 METERS
  BANDS 1-5, 7 30 METERS

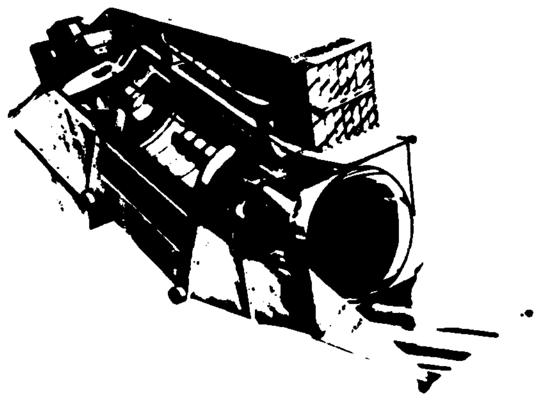

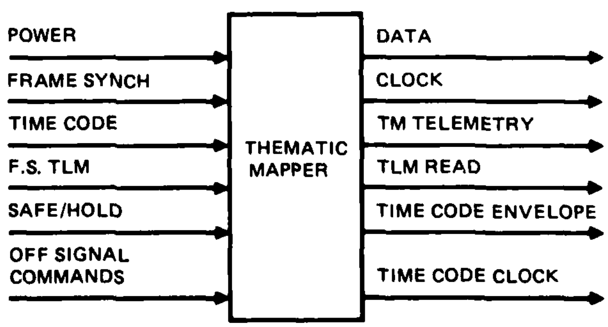

Figure 11. TM characteristics.

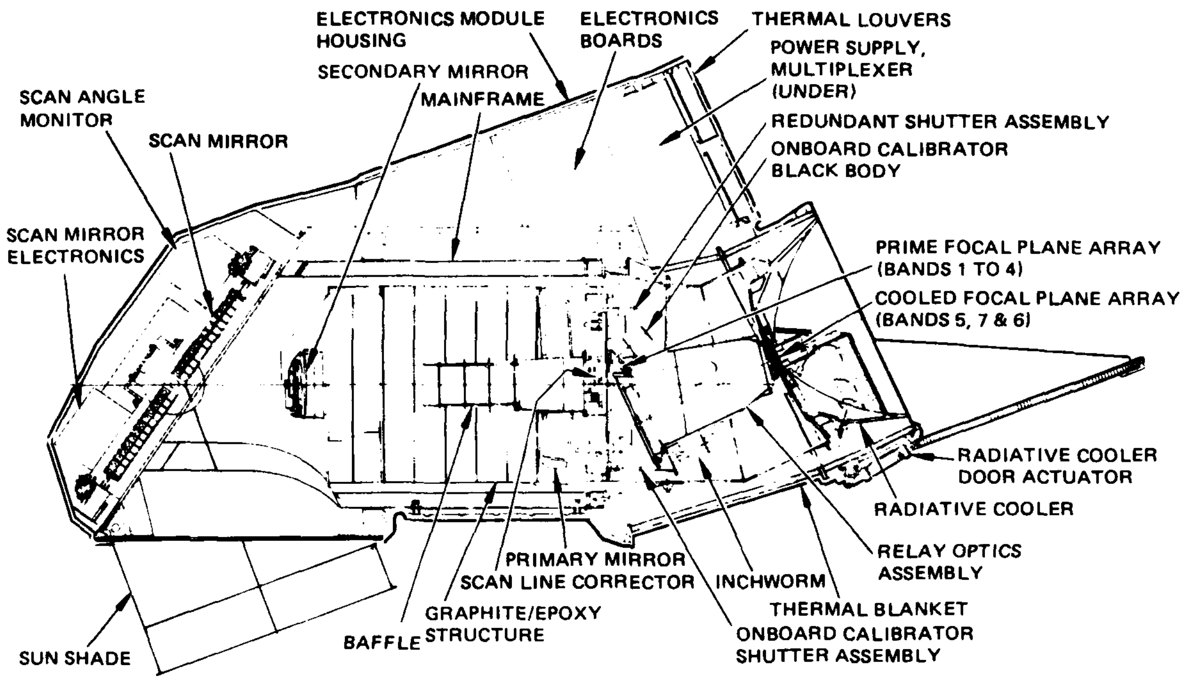

Figure 12. Cross-sectional view of TM.

LANDSAT Orbit	Near Polar, sun synchronous 705 km altitude 99 minute period 98.2° inclination angle 16-day repeat cycle
Scan	185 km swath 7 Hz rate
Optics	40.6 cm telescope aperture f/6 at prime focus 42.5 μrad IFOV, bands 1-4 f/3 at secondary focus (cooled) 43.8 μrad IFOV, bands 5, 7 170 μrad IFOV, band 6
Signal	8 bits/sample 52 kHz sampling rate, bands 1-5, 7 13 kHz sampling rate, band 6 1 sample/IFOV 85 Mbps multiplexed output

Table 15. Significant TM parameters.

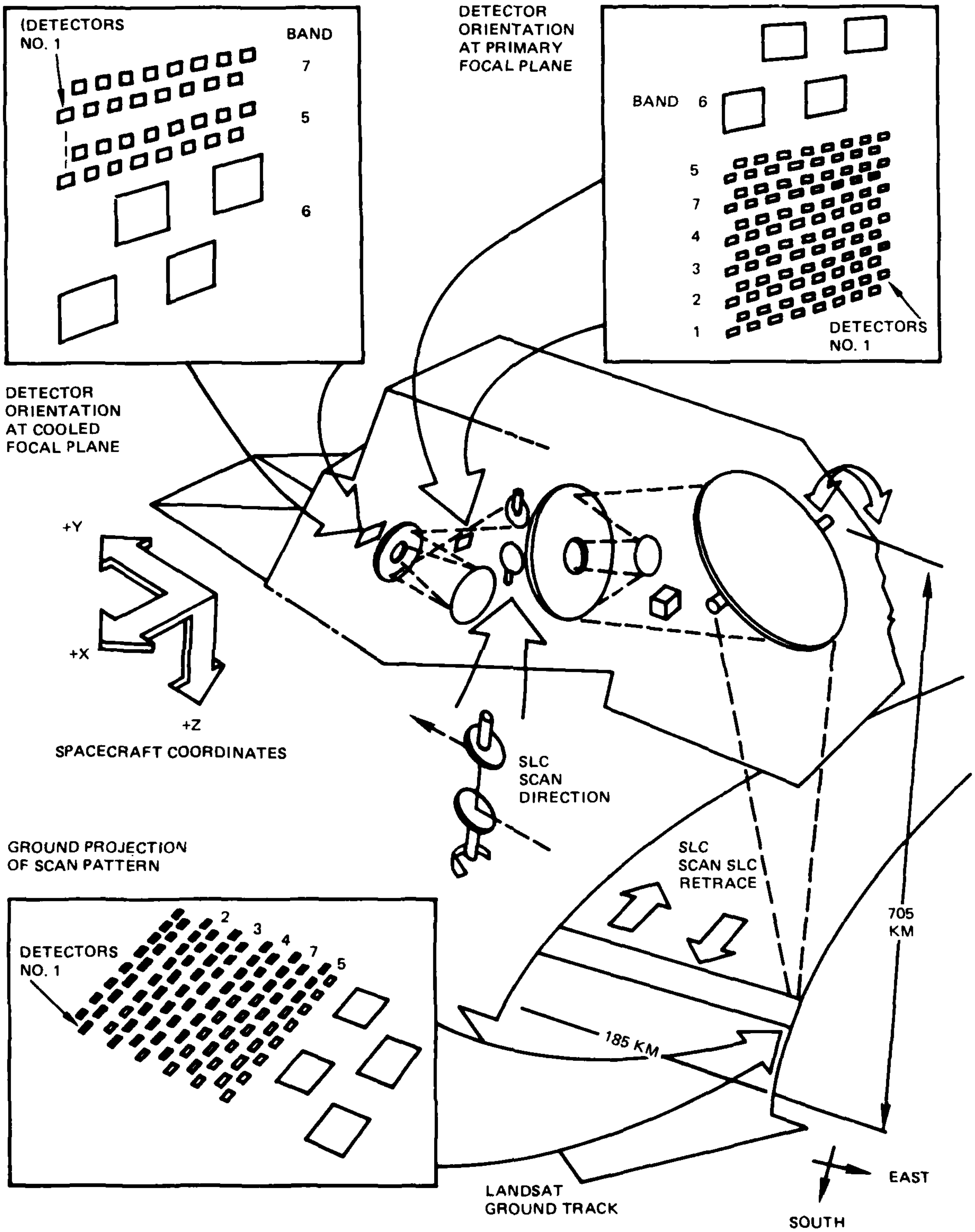

Figure 13. TM detector arrays.

Band	50% Response Lower Band Edge	Upper Band Edge
1	0.452 μm	0.518 μm
2	0.526	0.609
3	0.624	0.693
4	0.776	0.906
5	1.568	1.784
6	10.420	11.610
7	2.017	2.347

Table 16. Measured spectral response.

Table 17 summarizes the characteristics of the cooled focal plane assembly.

The cooled focal plane contains InSb detectors for bands 5 and 7. An (Hg Cd) Te type detector is used for band 6. Table 18 summarizes information on the detectors contained in the prime focal plane assembly.

The intended use of the various TM spectral pass bands is summarized in Table 19.

Number of bands	3
Number of detectors	
Bands 5.7 (monolithic InSb)	16/Band
Band 6 (photoconductive HgCdTe)	4
Detector size	
Bands 5, 7	0.0021 in. sq. (0.00533 cm sq)
Band 6	0.00816 in. sq. (0.0207 cm sq)
IFOV size	
Bands 5, 7	43.75 μrad
Band 6	170.0 μrad
Center-to-center spacing in each row	
Bands 5, 7	0.00408 in. (0.01036 cm) (2 IFOV)
Band 6	0.01632 in. (0.04145 cm) (2 IFOV)
Center-to-center spacing between rows	
Bands 5, 7	0.00510 in. (0.01295 cm) (2.5 IFOV)
Band 6	0.02040 in. (0.0518 cm) (2.5 IFOV)
Operating temperatures	90°K, 95°K, 105°K

Table 17. Cooled focal plane assembly.

Number of bands	4, Band Nos. 1 - 4
Number of detectors (monolithic silicon)	16/Band
Detector size	0.00408 in. sq. (0.01036 cm sq)
IFOV size	42.5 μrad
Band-to-band spacing	0.102 in. (0.259 cm) (25 IFOV)
Center-to-center spacing in each row	0.00816 in. (0.0207 cm) (2 IFOV)
Center-to-center spacing between rows	0.01020 in. (0.0259 cm) (2.5 IFOV)
Operating temperature	10° or 25°C

Table 18. Prime focal plane assembly.

Band	Range (μm)	Radiometric Resolution	Principal Applications
1	0.45-0.52	0.8 NEρ	Coastal water mapping *Soil/vegetation differentiation* Deciduous/coniferous differentiation
2	0.52-0.60	0.5% NEρ	Green reflectance by healthy vegetation
3	0.63-0.69	0.5% NEρ	Chlorophyll absorption for plant species differentiation
4	0.76-0.90	0.5% NEρ	Biomass surveys water body delineation
5	1.55-1.75	1.0% NEρ	Vegetation moisture measurement Snow/cloud differentiation
6	10.4-12.5	0.5K NETD	Plant heat stress management Other thermal mapping
7	2.08-2.35	2.4%NEρ	Hydrothermal mapping

Table 19. Spectral passbands and utilization.

3.1.6 SHUTTLE MULTISPECTRAL IR REFLECTANCE RADIOMETER (SMIRR)

SMIRR is a multispectral IR reflectance radiometer, designed for use aboard the "space shuttle." This is not a scanning (mapping) instrument, although it represents a precursor for instruments of that type. Engineering laboratory and aircraft flight tests have been carried out with SMIRR at the Jet Propulsion Laboratory (JPL) by J. F. Wellman and A. F. H. Goetz. Figure 14 depicts SMIRR, a multichannel visual/IR radiometer, equipped with bore-sighted film cameras.

It provides visual and IR measurements of the ground track radiance in 10 selected bands. The specific bands were selected for the detection and identification of surface mineralogic types. Table 20 lists the spectral bands.

Figure 15 shows the imaging spectrometer.

SMIRR consists of a 1.37 m focal length Cassegrain telescope, followed by a rotating filter, chopper wheel and a thermoelectrically cooled detector. An (Hg Cd) Te photoconductor, with a 3.5 μm cut-off is used for all spectral channels.

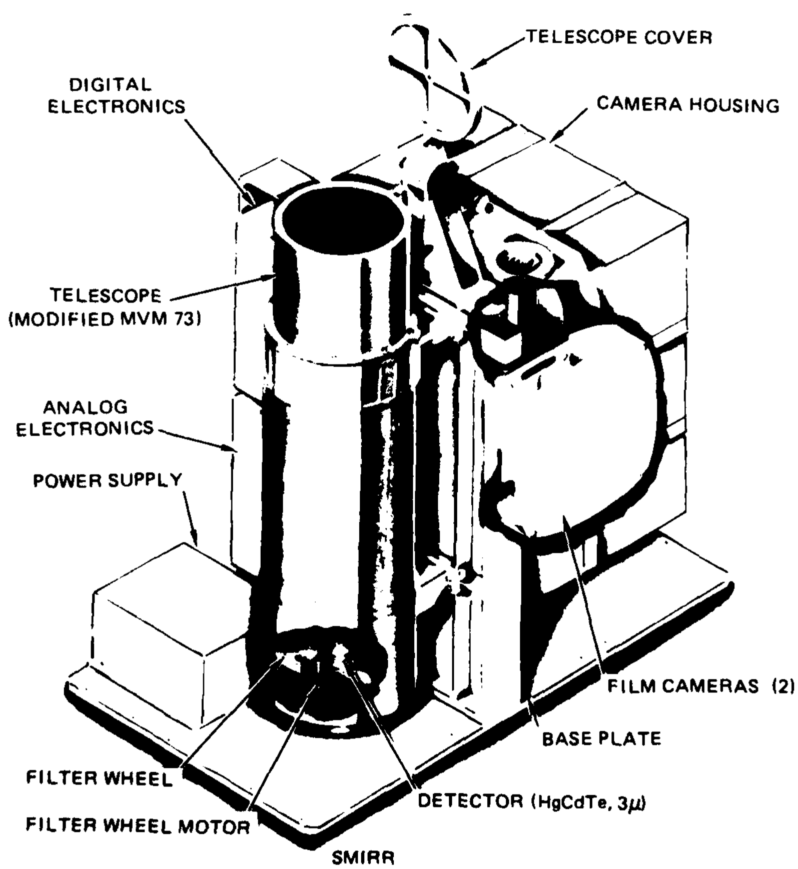

Figure 14. Shuttle multispectral infrared reflectance radiometer (SMIRR).

Channel	Center, μm	Half Power Bandwidth, μm
1	0.5 ± .02	0.1
2	0.6 ± .02	0.1
3	1.05 ± .02	0.1
4	1.2 ± .02	0.1
5	1.6 ± .02	0.1
6	2.1 ± .02	0.1
7	2.17 ± .005	0.02
8	2.20 ± .005	0.02
9	2.22 ± .005	0.02
10	2.35 ± .015	0.06

Table 20. Spectral bands for the SMIRR.

The imaging foreoptics are in an f/3 inverted Schwartzchild configuration with a folding flat to bring the image onto a source slit. Energy leaving the source slit passes through an aperture in the grating and is collimated by an f/3 paraboloid. The energy is then dispersed by the grating and reimaged by another f/3 paraboloid onto a 32 X 32 element area array detector contained in a demountable dewar. The grating is mounted on a set of swing arms (not shown) which permit it to be positioned at each of four angles with respect to the collimated beam, thereby selecting the subset of the full spectral range to be dispersed across the detector array. By stepping the mirror through a sequence of four steps per object line time, a total of 128 spectral lines is acquired with 32 spatial resolution elements per line. A spectral resolution of 0.01 μm is achieved.

The instrument electronics sample both signal and dark reference sections of the filter wheel. The dark reference values (associated with internal noise) are subtracted out, yielding corrected signal level values. Two 16 mm single-frame cameras, boresighted on the radiometer FOV, alternately acquire black and white images of the ground track for geographic reference.

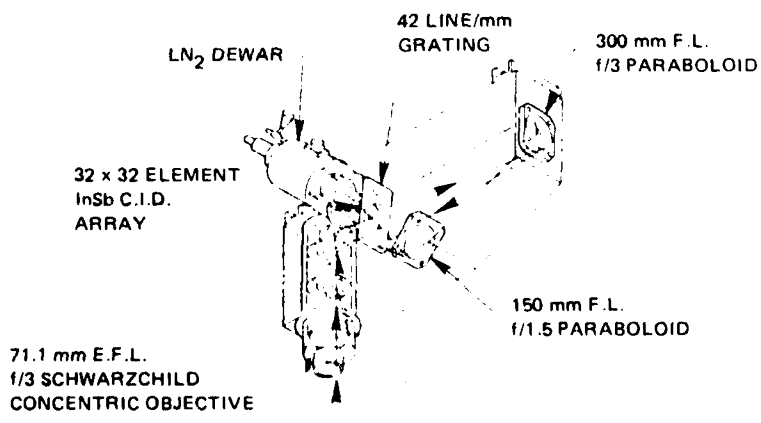

Figure 15. SMIRR spectrometer.

3.1.7 MULTISPECTRAL LINEAR ARRAY (MLA)

The MLA is envisioned as a follow-on multispectral scanning sensor to the TM in the LANDSAT series. It would operate in the so-called "pushbroom" scanning mode and thus provide much greater imaging times when viewing a given ground terrain pixel (picture element). This greater integration time (by a factor of 100 to 1000) results in a much improved S/N-ratio in the processed output. Figure 16 illustrates the geometry involved in the pushbroom scan technique. The detector array is composed of a set of independent detecting elements, aligned at right angles to the spacecraft projected upon the earth's surface.

The utilization of the pushbroom scan technique, in a multispectral array imager for an as yet undefined follow-on to LANDSAT D′, is presently in the very early concept formulation stage. The development of a "flyable" prototype version of the device is a long way "down the road," (possibly by 1990).

Preliminary concepts of multispectral, pushbroom scanning devices have been presented by A.A. Stark ("Multispectral Pushbroom Imager," AIAA Sensor Systems for the 80's, pp. 109-112, conference held at Colorado Springs, Co., 2-4 Dec. 1980) and by J.B. Wellman and F.H. Goetz ("Experiments in IR Spectral Mapping of Earth Resources," AIAA Sensor Systems for the 80's, pp. 163-174).

The simplified pushbroom scan detecting array illustrated in Figure 16 does not provide for spectral monitoring. Spectral monitoring could be achieved using a two dimensional detector array complex, in conjunction with a spectrum grating. Figure 17 depicts the concept.

The "swath direction" in Figure 17 is oriented at right angles to the satellite's track on the earth's surface. The spectral analysis is done with independent detector elements at right angles to the "swath" coordinate. The spectral analysis coordinate direction in the figure is designated (Red ← Wavelength → Blue).

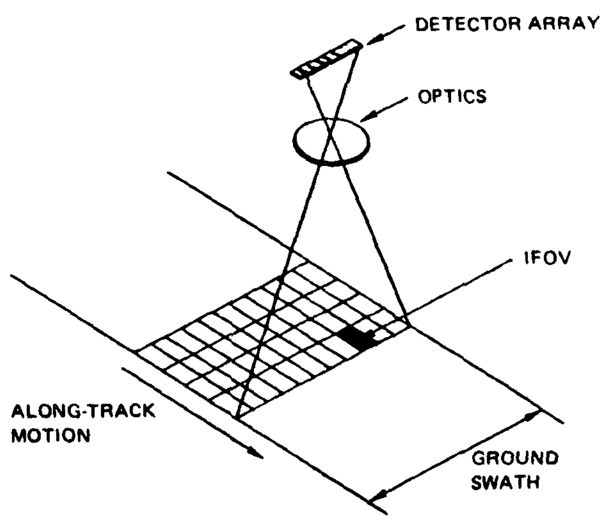

Figure 16. "Pushbroom" scan geometry.

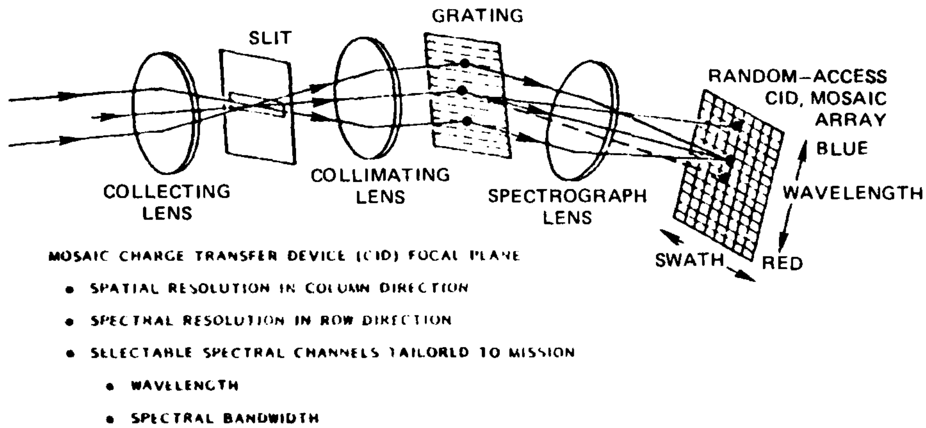

Figure 17. MLA sensor concept.

The outputs of the individual detector elements are read using a CID (Charge Injection Device) technique. The use of CID or CCD (Charged Coupled Device) image forming techniques is currently limited for the most part to MOS (Metal Oxide Silicon) structures. These photodiode arrays have a spectral energy gap cut-off in the neighborhood of 1.1 μm.

3.2 MICROWAVE SENSORS

Three microwave sensor devices will be discussed: (1) synthetic aperture radar (SAR), (2) microwave scatterometer (MS) and (3) scanning multichannel microwave radiometer (SMMR). The first two are active radar devices and the third is a passive microwave radiometer.

3.2.1 SYNTHETIC APERTURE RADAR (SAR)

SAR, in the form of an L-band radar, was operated aboard SEASAT-A during the latter part of 1978. SEASAT-A was the first dedicated experimental oceanographic satellite whose primary goal was to provide information on middle and large scale oceanic and atmospheric processes, e.g., ocean circulation, wind and wave patterns, etc.

The processing of coherent SAR returns greatly increases the achievable spatial resolution (with a given antenna beamwidth) in the direction parallel to the satellite motion. Good resolution in the direction at right angles to the satellite track can be achieved using standard pulse compression waveforms. SAR aboard SEASAT-A achieved spatial resolutions in both directions of approximately 25 m.

SEASAT-A operated in a near polar orbit at an altitude of 800 km. The SAR radar traced out a swath width of approximately 100 km. The operating frequency was centered in the neighborhood of 1.28 GHz. The average power was 55 watts. The antenna dish had an area of 25 m^2. A small portion of the recorded radar returns were digitally processed at JPL. SAR images can be processed using digital, optical correlators or CCD transverse filters. None of these techniques is easy to implement on a real-time basis. (See Radar Data Processing and Exploitation Facility by D.A. Ausherman et al in the proceedings of the IEEE 1977 International Radar Conference, Pub 75 CHO 938-1, AES, pp. 493-498.)

It is interesting to note that when LANDSAT-3 MSS images were combined with corresponding SEASAT-A/SAR digital data, the information content of the land cover maps was increased by 25 percent (Aviation Week and Space Technology, 29 September 1980, p. 65). The SAR data significantly increased the spatial resolution.

3.2.2 MICROWAVE SCATTEROMETER (MS)

An MS was operated aboard SEASAT-A to measure ocean surface wind speed and direction. The MS was a short pulse (4.8 ms) operating at 14.6 GHz. The radar return characteristics (Doppler shift) are a function of the surface wave motion (which in turn depends on the local wind speed and direction).

Figure 18 is a block diagram of the MS.

3.2.3 SCANNING MULTICHANNEL MICROWAVE RADIOMETER (SMMR)

SMMR devices were flown aboard NIMBUS-7 and SEASAT-A. SMMR senses the microwave thermal emission from the earth's surface and atmosphere and provides sea surface temperature and ocean surface wind speed data. It is pictured in Figure 19.

Figure 20 depicts the SMMR instrument configuration.

The SMMR instrument package consists of a radio frequency assembly, an electronics assembly, a power supply assembly and an antenna/scan mechanism assembly. The antenna/scan mechanism is mounted on the top of the spacecraft sensory ring. The remaining subassemblies are located in various bay sections within the sensory ring. The antenna, an offset parabolic reflector, points downward at an angle of 0.73 radian from nadir and scans ±0.44 radian (±25°) about the vertical nadir.

The MS achieved a spatial resolution of 50 km.

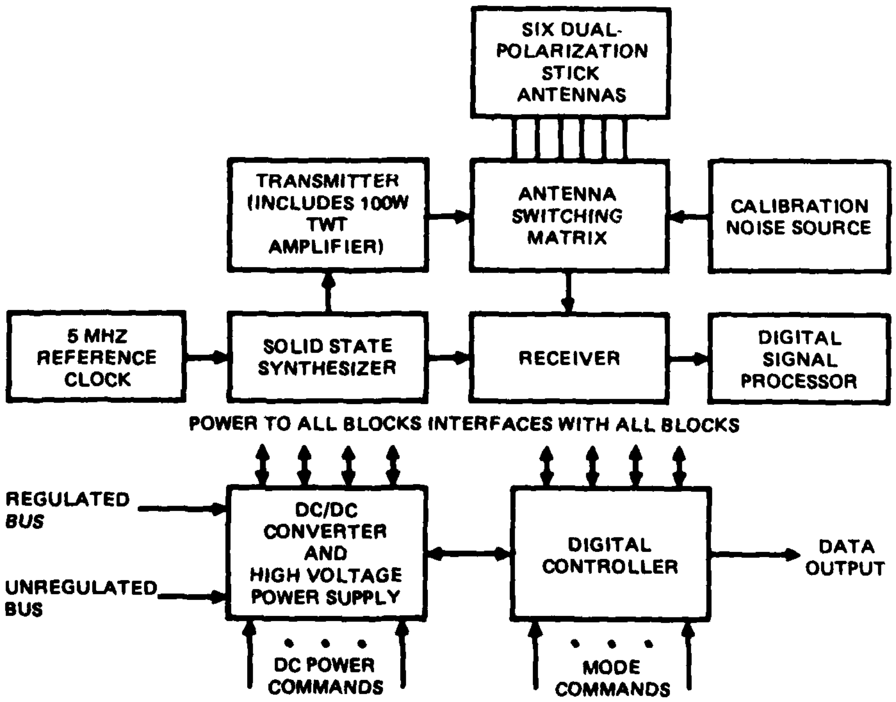

Figure 18. MS functional block diagram.

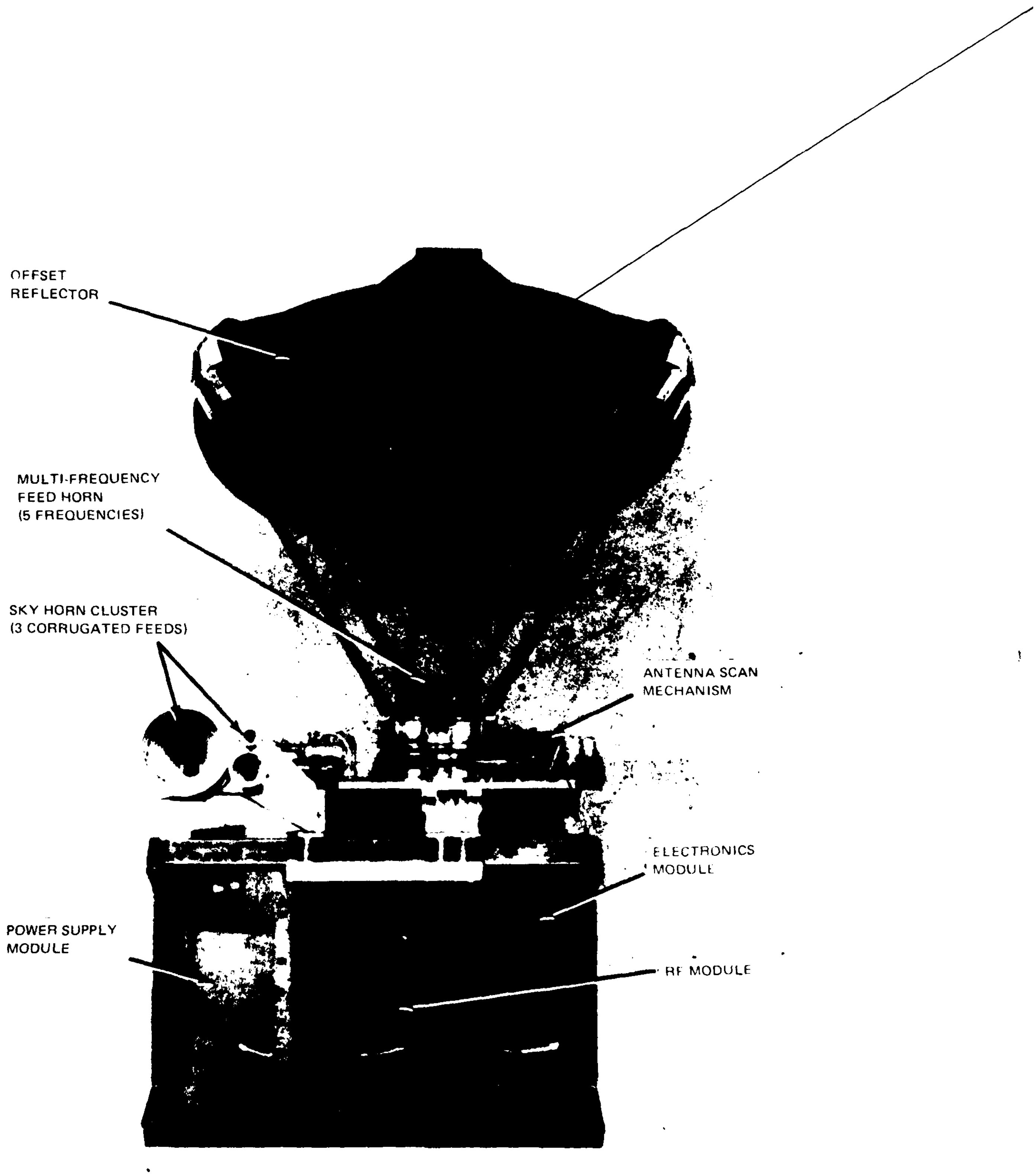

Figure 19. Scanning multichannel microwave radiometer (SMMR)

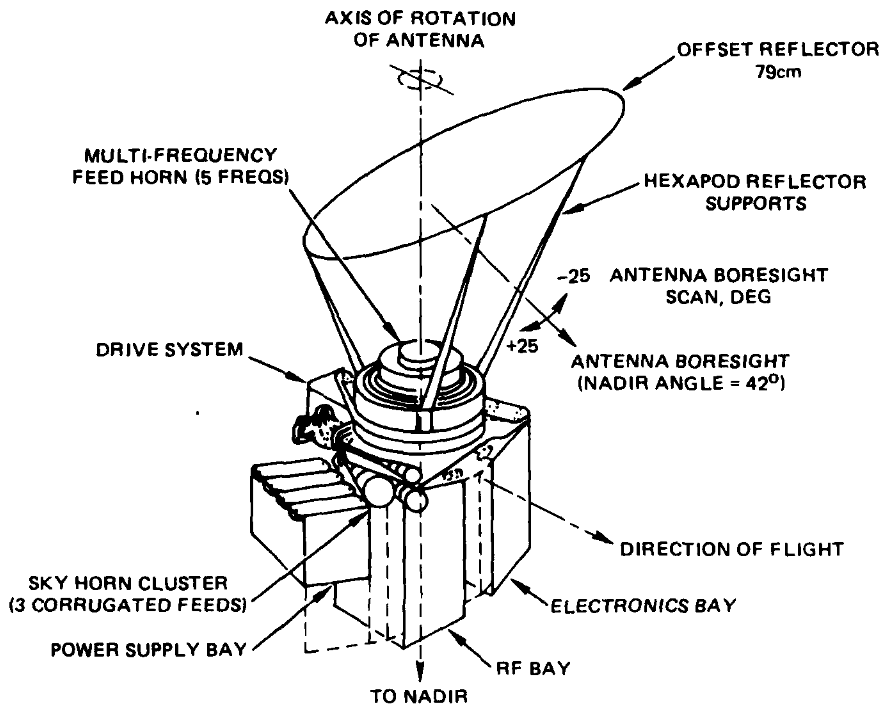

Figure 20. SMMR instrument configuration.

SMMR measures microwave thermal emissions from the earth's surface in five channels. Each channel monitors in two orthogonal linear polarizations.

Table 21 summarizes the SMMR performance parameters.

SMMR data from NIMBUS-7 and SEASAT-A indicate an agreement with "ground-truth" data for ocean surface temperatures of about 1° or 2°C. The actual measured "microwave brightness" is a function of the sea surface temperature, wind speed and salinity. The spatial resolution with SMMR is approximately 10 km. The swath width with the NIMBUS-7 spacecraft was approximately 780 km.

The SMMR sensor design characteristics are summarized in Table 22.

Figure 21 is a functional block diagram of MSSR.

Parameters	Channel				
	R1	R2	R3	R4	R5
Wavelength (cm)	4.0	2.8	1.7	1.4	0.8
Frequency (GHz)	6.633	10.69	18.0	21.0	37.0
RF bandwidth (MHz)	250	250	250	250	250
Integration time (msec) (approx)	126	62	62	62	30
IF frequency range (MHz)	10-110	10-110	10-110	10-110	10-110
Dynamic range (°K)	10-330	10-330	10-330	10-330	10-330
Absolute accuracy (°K rms)	<2.0	<2.0	<2.0	<2.0	<2.0
Temperature resolution, ΔT_{rms} (°K)	0.9	0.9	1.2	1.5	1.5
Antenna beamwidth (±0.1°)	4.4	2.75	1.65	1.32	0.77
Antenna beam efficiency (%)	87	87	87	87	87
Wavelength (cm)	4.54	2.80	1.66	1.43	0.81
Scan cycle (±25°) (seconds)	4.096	4.096	4.096	4.096	4.096
Double sideband noise figure (dB) (max.)	5.0	5.0	5.0	5.0	5.0

Table 21. SMMR performance parameters.

Item	Characteristics
Detectors:	RF diode – Dicke – superheterodyne
Size:	Two 15.3 - by 33.0 - by 20.4-cm modules (two NIMBUS bays) One 15.3- by 16.5- by 20.4-cm module (one-half NIMBUS bay) Parabolic section antenna, 80 cm in diameter Multifrequency antenna feed
Weight:	52.3 kg
Power:	60 watts
Commands:	12
Data:	DAPS – 2 kbs(1)
Telemetry:	Digital B – 9(2)
	Analog – 19
Clock:	Time code Strobe 1 Hz 10 kHz 1.6 MHz

(1) NIMBUS 7 data processing
(2) Lower data rate in DAPS for collecting digital words

Table 22. SMMR sensor design characteristics.

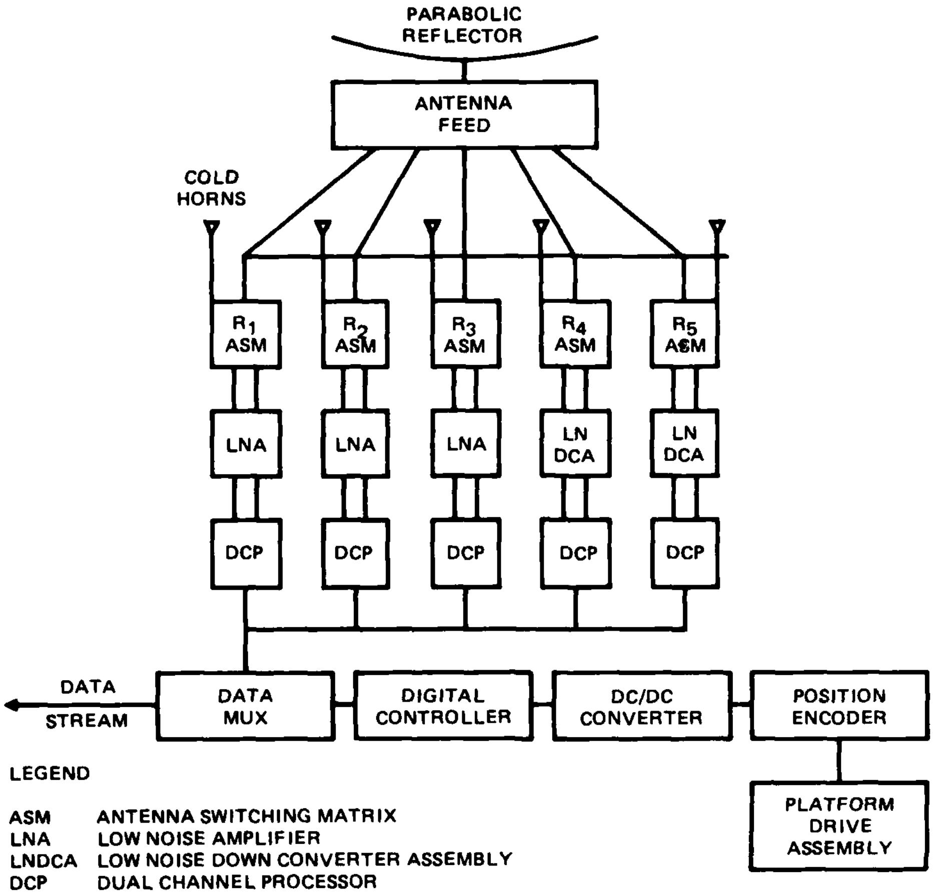

Figure 21. MSSR functional block diagram.

4.0 CONCLUSIONS AND RECOMMENDATIONS

An extensive body of knowledge and operating experience exists within NASA and NOAA concerning the development and utilization of satellite-borne non-DoD imaging sensors for terrestrial observations. It is most likely that some of this civilian technical knowledge and operational experience could be utilized profitably in the planning and development of future military satellite systems. Table 23 lists the initial launch dates of various civilian satellite series of primary interest.

Sensors of primary interest related to the Naval Ocean Surveillance mission are:

- SAR
- MSS
- TM
- MLA
- SMMR

Satellite Type	Initial Launch (Year)
TIROS	1960
ESS (Environmental Survey Satellite)	1960
ITOS/NOAA	1970
LANDSAT	1972
GOES	1974
DMSP	1976
SEASAT	1978

Table 23. Initial launch year for satellite types.

To usefully exploit the summary data and information contained in the present report, it is recommended that a "small-scale" (1 man-year) program be initiated. The recommended program consists of the following three elements:

(1) In depth review and analysis of literature concerning satellite sensor systems, including military systems

(2) Visitation and discussion with resident experts at GSFC, LaRC, JPL, APL, NOAA, SIO, EROS, SAMSO, etc., to obtain latest relevant information and examples of sensor products

(3) Summary report

APPENDIX A
BIBLIOGRAPHY

1. Remote Sensing: New Eyes to See the World, National Geographic Magazine, Washington, DC., January 1969.
2. Skylab: Its View of Earth. National Geographic Magazine, Washington, DC., October 1974.
3. The EROS Data Center, United States Department of Interior Geological Survey, EROS Data Center, Sioux Falls, South Dakota 57198, 1972.
4. United States Activities in Spacecraft Oceanography, National Council on Marine Resources and Engineering Development, Superintendent of Documents, Washington, DC., No. P.E. 12.2: SP1, 1967.
5. ERTS: Activities Related to Earth Resources. National Aeronautics and Space Administration, Washington, DC., 1974.
6. Yentsch, C.S., The Absorption and Fluorescence Characteristics of Biochemical Substances in Natural Waters, Proceedings of Symposium on Remote Sensing in Marine Biology and Fisheries, March 1971 (Texas A&M University, College Station, 1971), pp 75-97.
7. Clarke, G.L., The Significance of Spectral Changes in Light Scattered by the Sea in Remote Sensing in Ecology (University of Georgia Press, Athens, 1969), Chap. 11.
8. Hovis, W.A., Forman, M.L. and Blaine, L.R., Detection of Ocean Color Changes from High Altitude, NASA X-652-73-371, November 1973.
9. Smith, R.C. and Baker, K.S., The Bio-Optical State of Ocean Waters and Remote Sensing, Scripps Institution of Oceanography, Ref. 77-2 (1977).
10. Smith, R.C. and Baker, K.S., Optical Classifications of Natural Waters, Scripps Institution of Oceanography, Ref. 77-4, (1977).
11. NESS (National Environmental Satellite Service) 57 Nimbus-5 Sounder Data Processing System, Part I: Measurement Characteristics and Data Reduction Procedures, W.L. Smith, H.M. Woolf, P.G. Abel, C.M. Hayden, M. Chalfant, and N. Grody, June 1974, 99 pp (COM-74-11436/AS).
12. NESS 59 Use of Geostationary – Satellite Cloud Vectors to Estimate Tropical Cyclone Intensity, Carl O. Erickson, September 1974, 37 pp (COM-74-11762/AS).
13. NESS 60 The Operation of the NOAA Polar Satellite System, Joseph J. Fortuna and Larry N. Hambrick, November 1974, 127 pp (COM-75-10390/AS).
14. NESS 61 Potential Value of Earth Satellite Measurements to Oceanographic Research in the Southern Ocean, E. Paul McClain, January 1975, 18 pp (COM-75-10479/AS).
15. NESS 64 Central Processing and Analysis of Geostationary Satellite Data, Charles F. Bristol (Editor), March 1975, 155 pp (COM-75-10853/AS).
16. NESS 65 Geographical Relations Between a Satellite and a Point Viewed Perpendicular to the Satellite Velocity Vector (Side Scan), Irwin Ruff and Arnold Gruber, March 1975, 14 pp (COM-75-10678/AS).

17. NESS 66 A summary of the Radiometric Technology Model of the Ocean Surface in the Microwave Region, John C. Alishouse, March 1975, 24 pp (COM-75-10849/AS).

18. Sensor Systems for the 80's – Conference, AIAA publication at USAFA Conference, Colorado Springs, Colorado (2-4 December 1980).

19. Remote Sensing of Earth From Space: Role of 'Smart Sensors' AIAA Publication Volume 67.

20. Hovis, W.A., et al, Nimbus-7 Coastal Zone Color Scanner: System Description and Initial Imagery, Science Vol. 210, 1980, pp 60-63.

21. Phinney, D.D.; Stuff, R.G.; Houston, A.G.; Hsu, E.M.; and Trenchard, M.H.; Accuracy and performance of LACIE Yield Estimates in Major Wheat Producing Regions of the World, Proceedings of the LACIE Symposium, Vol. I, Johnson Space Center, pp 589-605.

22. Blanchard, L.E., and Weinstein, Oscar, Design Challenges of the Thematic Mapper. Volume 18, Number 2 of IEEE Transactions on Geoscience and Remote Sensing.

23. Helton, M.R., Software Requirements for SEASAT Footprint Location, Jet Propulsion Laboratory -- EM 312/77-23, February 1, 1977.

24. Wu, C., A Digital Fast Correlation Approach to Produce SEASAT SAR Imagery, IEEE International Radar Conference, Arlington, VA., April 28-30, 1980.

25. Gordon, H.R., and Hars, W.A., Phytoplankton Pigments from the Nimbus-7 Coastal Zone Color Scanner: Comparisons with surface Measurements, Science Vol. 210, 1980, pp 63-66.

26. Goetz, A.F.H. and Rowan, L.C., Geologic Remote Sensing, Science, in press, 1980.

27. Goetz, A.F.H., et al: Application of ERTS images and image processing to regional geologic problems and geologic mapping in northern Arizona, Jet Propulsion Laboratory Tech Report 32-1597, 1975.

28. Gibbons, M.D.; Swab, J.M.; Davern, W.E.; and Aldrich, R.W., Performance Efficiency of InSb Charge Injection Devices (CID), Proceedings of Society of Photo-Optical Instrumentation Engineers, Vol. 203, August 1979, pp 158-165.

29. Wellman, J.B., and Norris, D.D., Onboard Processing for Future Space-Borne Imaging Systems, in Remote Sensing of the Earth from Space: Role of "Smart Sensors," R.A. Breckenridge, ed., Vol. 67, Progress in Astronautics and Aeronautics, Vol. 67, 1979.

30. Multispectral Linear Array Phase A Final Report Jet Propulsion Laboratory Internal Document 715-82, November, 1980.

31. Norris, D.D., and Wellman, J.B., Earth-Sensing Technology, 1980 Government Microcircuit Applications Conference (Houston, Texas), 19-21 November 1980.

32. CCD Applications to SAR, Proceedings of CCD 175, 1975 International Conference on the Application of Charge-Coupled Devices, 29-31 October 1975 at NELC, San Diego, California, pp 301-308.

    CID Imaging – Present Status and Opportunities, pp 93-99.

    A High Performance 190X 244 CCD Area Image Sensor Array, pp 101-108.

    A CCD Memory for Radar Signal Processing, pp 413-420.

33. Execution Phase Project Plan for National Oceanic Satellite System (NOSS). NASA GSFC, preliminary version document, dated July 1980.

34. General Electric Co., Space Division., NIMBUS-7, Reference Manual.

35. The Potential of Spaceborne Synthetic Aperture Radar for Oceanography, Johns Hopkins APL Technical Digest, June 1980, Vol. 1, No. 2, pp 148-156.

36. The NIMBUS-7 Users' Guide, NASA GSFC, August 1978.

37. TIROS-N/NOAA A-G Satellite Series, NESS TM95, March 1978.

38. "NOAA-B" NASA GSFC, 1980.

39. Data Extraction and Calibration of TIROS-N/NOAA Radiometers, NESS TM 107, November 1979.

40. NIMBUS: The Vanguard of Remote Sensing, IEEE Spectrum, November 1978, pp 36-43.

41. DARPA Unveils Staring Focal Plane Array, Defense Electronics, October 1980, pp 101-113.

42. Aviation Week and Space Technology:

    TIROS-N Performance Gains, 21 July 1980, p 51.

    New Satellite (GOES) To Sample Data on Weather, 15 September, 1980, pp 24-25.

    Free Enterprise and LANDSAT, 14 July 1980, p 13.

    Outlook Brightens for Thematic mapper (TM), 29 September, 1980, pp 65-66.

    Two-Step Operational LANDSAT Plan Set, 14 July 1980, pp 108-115.

    LANDSAT Woes, 11 August 1980, p 17.

    LANDSAT-2 Returned to Active Use, 30 June 1980, p 58.

    LANDSAT Thematic Mapper Model in Test, 14 July 1980, p 117.

    Mapping Specialists and Geologists are Continuing to Press NASA for Placement of Return-Beam VIDICON Cameras on the LANDSAT D Spacecraft, 1 August 1980, p 15.

    Problems Force LANDSAT D Restructure, 9 June 1980, pp 20-22.

43. The TIROS-N Twins are Coming, NOAA Reprint Vol. 8, No. 2, April 1978.

APPENDIX B

PERSONS AND ORGANIZATIONS

(from whom information was obtained to be utilized in this study)

Frank Barath, Jet Propulsion Laboratory (JPL)

R.A. Beckenridge, NASA, LaRC

Dr. R.L. Bernstein, SIO, Visibility Laboratory

Dr. J.L. Engel, Hughes, Santa Barbara Research Center

Joseph Fuller, Jr., NASA, GSFC

Dr. P. Gloersen, NASA, GSFC

Dr. A.F.H. Goetz, JPL

Dr. M.P. Guberek, SIO, (Satellite Remote Sensing Facility)

Dr. W.A. Hovis, Jr., NOAA NESS Code S-32, Room 0135, FOB 4, Washington, D.C.

Al Jones, NASA, GSFC

Robert Jones, Hughes Aircraft Company, Space and Communications Group

Norman Ortwein, Naval Ocean Systems Center (NOSC)

Dr. H. Plotkin, NASA, GSFC, Code 940

Dr. Dan Schneiderman, JPL

Dr. V. Solomonson, NASA, GSFC, Code 920

Dr. J.M.F. Vickers, JPL

Dr. F.O. Von Bun, NASA, GSFC, Code 900

Oscar Weinstein, NASA, GSFC

Jim Welch, NASA Headquarters

Dr. J.B. Wellman, JPL

K.P. White, III, Aerospace Corporation

Del P. Williams, III, NASA Headquarters

Dr. Robert Wringley, NASA AMES Research Center

Dr. C. Wu, JPL

Dr. Charles Yentsch, Bigelow Laboratory of Ocean Sciences, West Boothbay Harbor, Maine

APPENDIX C
EM SPECTRUM AND ATMOSPHERIC TRANSMISSION CHARACTERISTICS

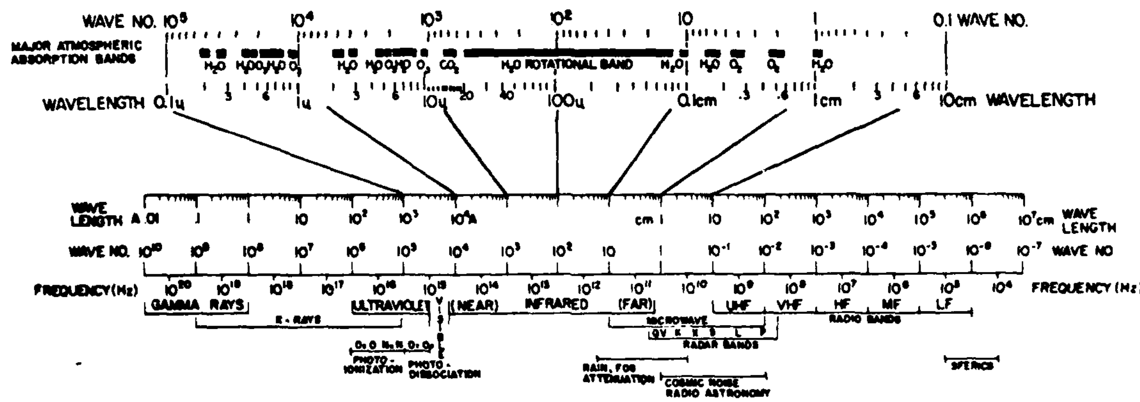

APPENDIX D

SEASAT-SAR IMAGES

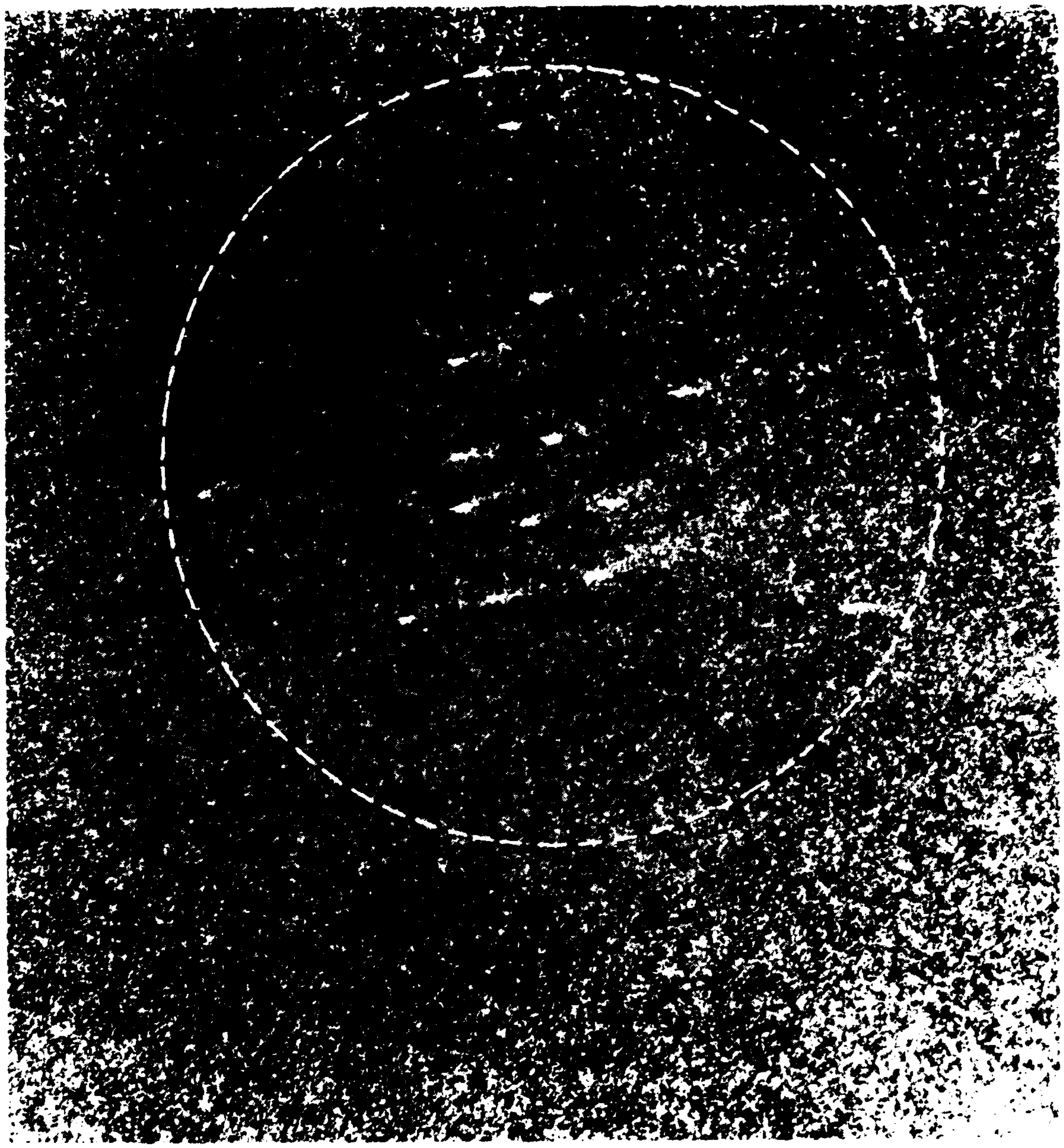

Figure 22. NATO task force in Irish Sea

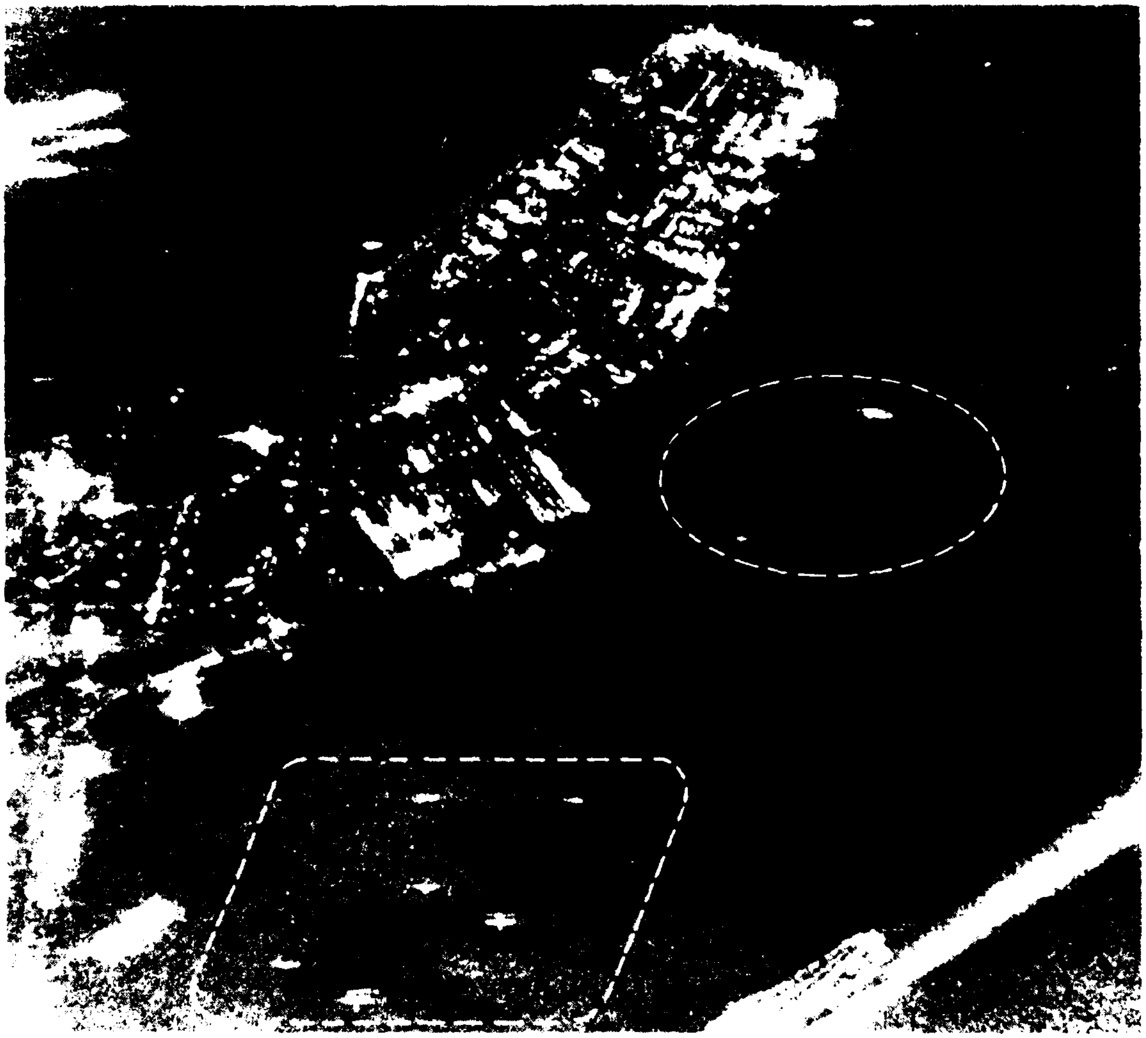

Figure 23. Ships in San Francisco bay

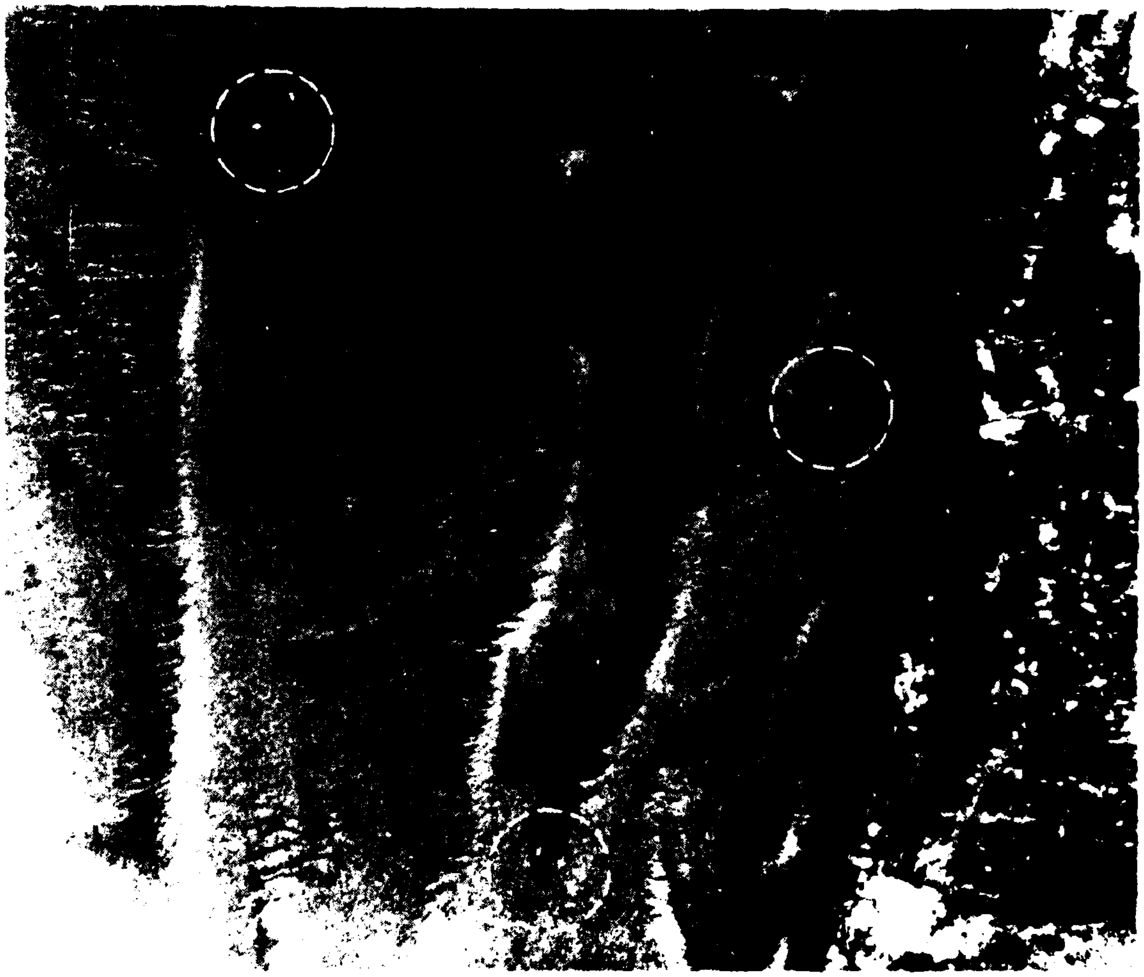

Figure 24. Small craft off French coast in English Channel

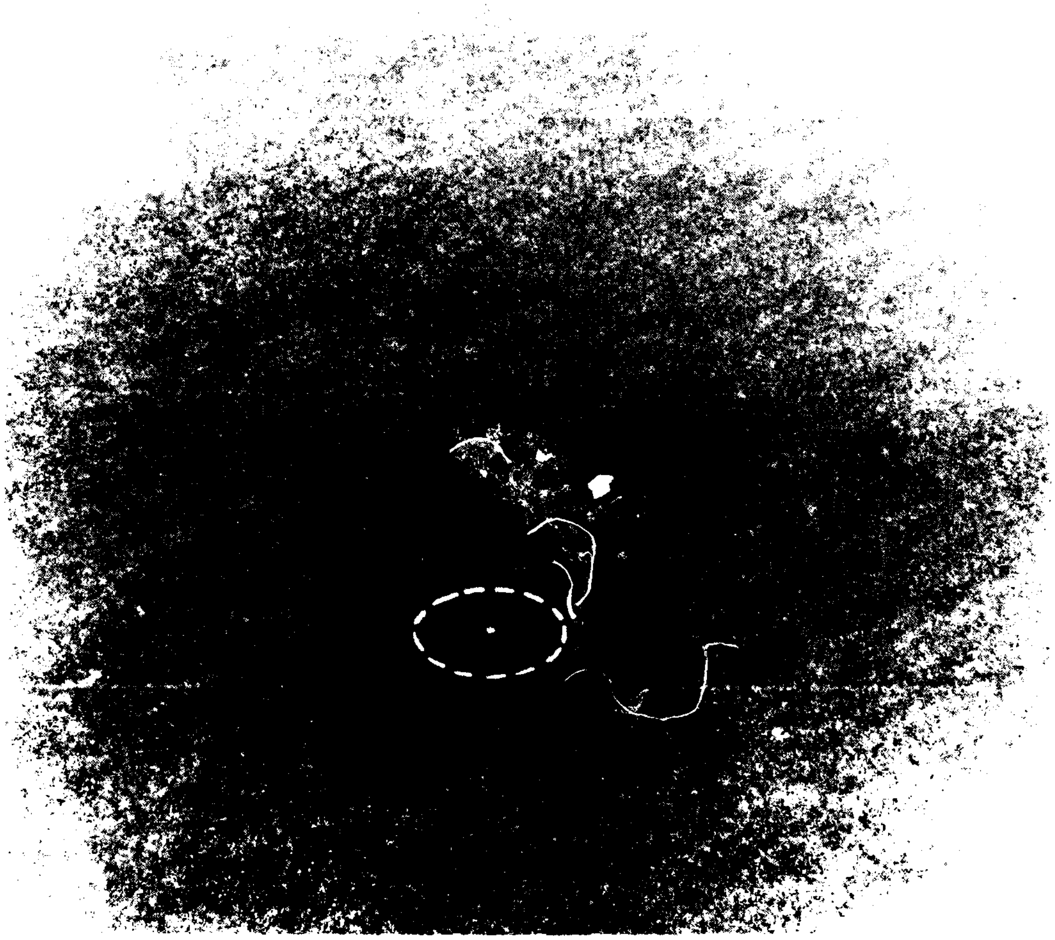

Figure 25. Oceanography vessels in Gulf of Alaska

APPENDIX E

LANDSAT IMAGES IN SHIPPING

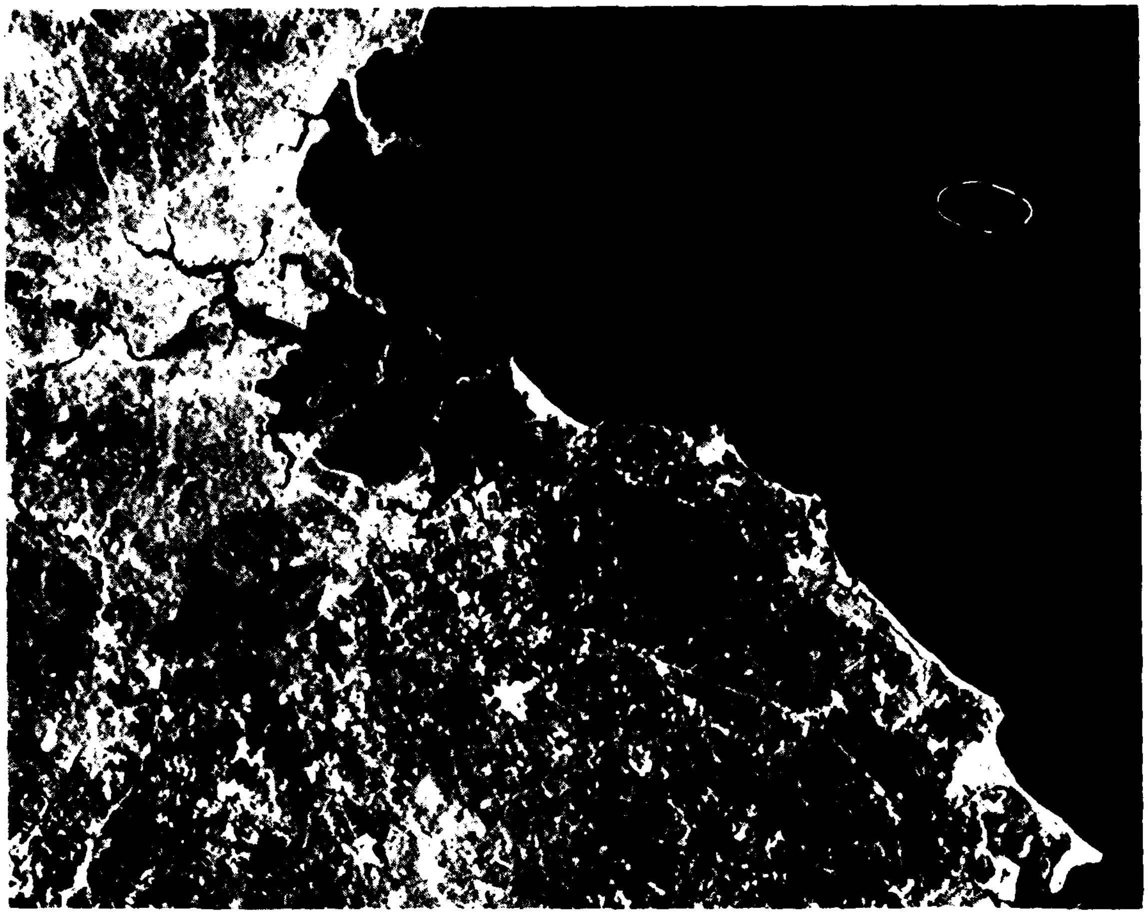

Figure 26. Shipping off of Boston

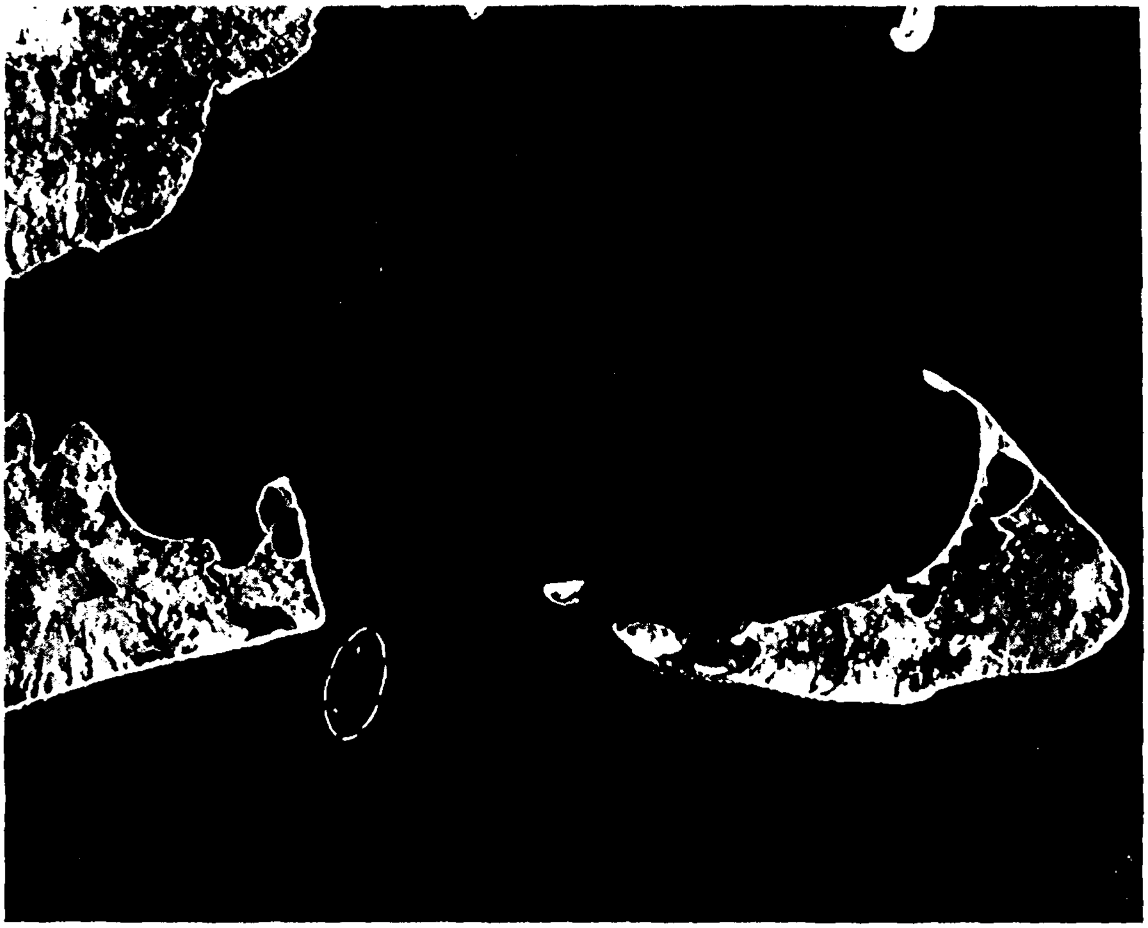

Figure 58. Shipping off of New York City

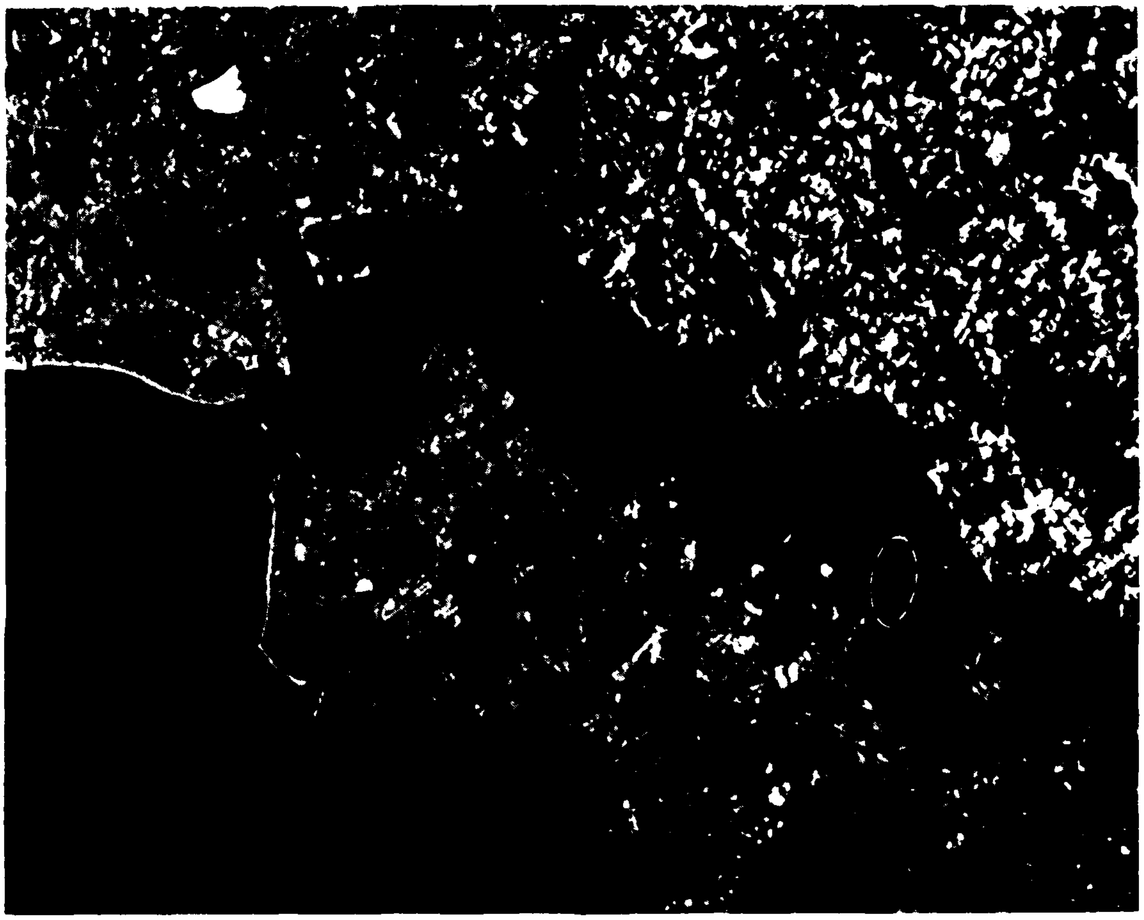

Figure 29. Shipping near Norfolk, Virginia

DAT

FILM

2-